LUND UNIVERSITY

Proton-Conducting Sulfonated Aromatic Ionomers and Membranes by Chemical Modifications and Polycondensations

Persson Jutemar, Elin

2010

Proton-conducting sulfonated aromatic ionomers and membranes by chemical modifications and polycondensations

Elin Persson Jutemar

Division of Polymer & Materials Chemistry

Thesis
2010

LUND UNIVERSITY

Thesis submitted for the degree of Doctor of Philosophy in Engineering, to be defended in public at the Center for Chemistry and Chemical Engineering, Lecture Hall K:C, on December 15, at 10.00, as approved by the Faculty of Engineering, Lund University
Opponent: Professor Howard M. Colquhoun
Department of Chemistry, University of Reading, United Kingdom

Organization	Document name
LUND UNIVERSITY Division of Polymer & Materials Chemistry Lund Institute of Technology P. O. Box 124 SE-221 00, Sweden	DOCTORAL DISSERTATION
	Date of issue 2010-12-15
	Sponsoring organization Swedish Foundation for Strategic Environmental Research, MISTRA
Author(s) Elin Persson Jutemar	

Title and subtitle Proton-conducting sulfonated aromatic ionomers and membranes by chemical modifications and polycondensations

Abstract

Proton-exchange membrane fuel cells (PEMFC)s are increasingly regarded as promising environmentally benign power sources. Intensive development is today directed towards reducing the cost and increasing the durability of the fuel cell, as well as expanding the operational window for the PEMFC for a range of applications. The proton-conducting membrane is one of the key components in the PEMFC. The need for improved performance of the proton-conducting membrane has led to an extensive worldwide research, from which aromatic ionomers have emerged as promising candidates. One of the major challenges is to prepare functional high-performance proton-conducting membranes, with optimized properties. By concentrating the sulfonic acid groups, which facilitate the proton transport, to specific chain segments, the nanophase separation between hydrophilic and hydrophobic domains may be enhanced, which may provide membranes with balanced water sorption characteristics.

In the present work, the sulfonic acid groups were concentrated to specific segments in either the polymer backbone or on pendant side chains. Based on the former approach, polysulfones with fully tetrasulfonated aryl-SO_2-aryl-aryl-SO_2-aryl segments were prepared by lithiation, reaction with sulfur dioxide, followed by oxidation of the resulting sulfinates. The possibility to fully tetrasulfonated these segments offer possibilities to prepare various aromatic copolymers and membranes with locally very high densities of hydrolytically stabile sulfonic acid groups.

As a second approach to enhance the phase separation, the sulfonic acid groups were separated from the polymer backbone and were concentrated to side chains. PSUs carrying various mono-, di - and trisulfonated side chains were synthesized by chemical modification. Moreover, aromatic ionomer with various polymer backbones with pendant benzoyl side chains were synthesized by polycondensations. SAXS measurements showed that longer side chains and higher local acid concentrations, gave larger characteristic separation length between the ionic clusters accompanied with narrower distribution. Proton conductivity measurements showed that larger characteristic separation lengths resulted in higher proton conductivities. The ionic clustering of ionomers bearing sulfobenzoyl side chains was shown to be promoted by ionomers with flexible polymer backbones, which subsequently resulted in higher proton conductivity, but with the drawback of having lower thermal stability. The water uptake characteristics in the ionomers bearing sulfobenzoyl side chains was efficiently controlled by incorporating non-sulfonated comonomers.

Key words: Ionomers, Polyaromatics, Polycondensation, Polymer electrolytes, Proton conductivity, Proton-exchange membrane fuel cells, Sulfonation, Sulfonated monomers, Sulfonated polymer electrolytes, X-ray scattering

Classification system and/or index termes (if any):

Supplementary bibliographical information:		Language English
ISSN and key title:		ISBN 978-91-7422-255-5
Recipient's notes	Number of pages 136	Price
	Security classification	

Proton-conducting sulfonated aromatic ionomers and membranes by chemical modifications and polycondensations

Elin Persson Jutemar

2010

Doctoral thesis

Division of Polymer & Materials Chemistry
Lund University
P.O. Box 124, SE-22100 Lund, Sweden

ISBN 978-91-7422-255-5

Printed by MediaTryck AB, Lund

LIST OF PAPERS

This thesis is the result of studies presented in the following papers, referred to in the text by their respective Roman numerals.

I. **Sulfonated poly(arylene ether sulfone) ionomers containing di- and tetrasulfonated arylene sulfone segments**
Elin Persson Jutemar, Shogo Takamuku, and Patric Jannasch
Manuscript accepted for publication in Polymer Chemistry
DOI:10.1039/c0py00290a.

II. **Locating sulfonic acid groups on various side chains to poly(arylene ether sulfone)s: Effects on the ionic clustering and properties of proton-exchange membranes**
Elin Persson Jutemar and Patric Jannasch
Journal of Membrane Science 2010, 351, 87-95.

III. **Facile Synthesis and Polymerization of 2,6-Difluoro-2'-sulfobenzophenone for Aromatic Proton Conducting Ionomers with Pendant Sulfobenzoyl Groups**
Elin Persson Jutemar, Shogo Takamuku, and Patric Jannasch
Macromolecular Rapid Communications 2010, 31, 1348-1353.

IV. **Influence of the Polymer Backbone Structure on the Properties of Aromatic Ionomers with Pendant Sulfobenzoyl Side Chains for Use as Proton-Exchange Membranes**
Elin Persson Jutemar and Patric Jannasch
Manuscript submitted to ACS Applied Materials & Interfaces

V. **Copoly(Arylene Ether Nitriles) and Copoly(Arylene Ether Sulfone) Ionomers with Pendant Sulfobenzoyl Groups for Proton Conducting Fuel Cell Membranes**
Elin Persson Jutemar and Patric Jannasch
Manuscript accepted for publication in Journal of Polymer Science, Part A: Polymer Chemistry

ADDITIONAL PAPER NOT INCLUDED IN THE THESIS

Pore Size Distribution and Water Uptake in Hydrocarbon and Perfluorinated Proton-Exchange Membranes as Studied by NMR Cryoporometry
S. von Kraemer, A. I. Sagidullin, G. Lindberg, I. Furó, E. Persson, and P. Jannasch
Fuel Cells 2008, 08, 262-269.

MY CONTRIBUTION TO THE PAPERS

Paper I: I took an active part in the planning of the study. I performed all the experimental work except for the polymerizations. I wrote the paper.

Paper II: I took an active part in the planning of the study. I performed all the experimental work and wrote the paper.

Paper III: I took an active part in the planning of the study. I performed all the experimental work except for the polymerizations. I wrote the paper.

Paper IV: I took an active part in the planning of the study. I performed all the experimental work and wrote the paper.

Paper V: I took an active part in the planning of the study. I performed all the experimental work and wrote the paper.

ABBREVIATIONS

BCPSB	4,4'-Bis[(4-chlorophenyl)sulfonyl]-1,1'-biphenyl
DCDPS	Dichlorodiphenyl sulfone
DFSBP	2,6-Difluoro-2'-sulfobenzophenone lithium salt
DL	Degree of lithiation
DMAc	*N,N*-Dimethylacetamide
DMFC	Direct methanol fuel cell
DMSO	Dimethylsulfoxide
EIS	Electrochemical impedance spectroscopy
EW	Equivalent weight
FTIR	Fourier transform infrared spectroscopy
IEC	Ion-exchange capacity
n-BuLi	*n*-Butyllithium
NMP	*N*-Methyl pyrrolidone
NMR	Nuclear magnetic resonance spectroscopy
PAE	Poly(arylene ether)
PAEES	Poly(arylene ether ether sulfide)
PAEN	Poly(arylene ether nitrile)
PAES	Poly(arylene ether sulfone)
PAS	Poly(arylene sulfide)
PEEK	Poly(ether ether ketone)
PEMFC	Polymer electrolyte membrane fuel cell or Proton-exchange membrane fuel cell

PSU	Polysulfone
RH	Relative humidity
SAXS	Small angle X-ray scattering
SBACA	2-Sulfobenzoic acid cyclic anhydride
SBFBB	1,4-Bis(3-sodium sulfonate-4-fluorobenzoyl) benzene
SDCDPS	Disodium 3,3-disulfonate-4,4'-dichlorodiphenyl sulfone
SDFBP	Disodium 3,3-disulfonate-4,4'-difluorobenzophenone
sPEEK	Sulfonated poly(ether ether ketone)
T_d	Degradation temperature
T_g	Glass transition temperature
THF	Tetrahydrofuran

CONTENTS

Scope of the work ..... - 1 -

Introduction ..... - 3 -

2.1 Proton-exchange membrane fuel cells ..... - 3 -

2.2 Proton-conducting polymer membranes ..... - 5 -

Polymer synthesis and chemical modification ..... - 15 -

3.1 Characteristics of polysulfones ..... - 15 -

3.2 Direct sulfonation of polysulfones ..... - 16 -

3.3 Lithiation of polysulfones ..... - 17 -

3.4 Nucleophilic aromatic substitution reactions ..... - 19 -

3.5 Random copolymerization ..... - 21 -

Special characterization techniques ..... - 25 -

4.1 Small angle X-ray scattering (SAXS) ..... - 25 -

4.2 Proton conductivity measurements ..... - 26 -

Thesis work ..... - 29 -

5.1 Polysulfones carrying highly sulfonated segments (Paper I) ..... - 33 -

5.2 Polysulfones carrying sulfonated aromatic side chains (Paper II) ..... - 38 -

5.3 Aromatic homopolymers and copolymers with pendant sulfonated side chains prepared by polycondensation reactions (Papers III-V) ..... - 42 -

Summary and outlook ..... - 51 -

Populärvetenskaplig sammanfattning ..... - 53 -

Acknowledgements ..... - 55 -

References ..... - 57 -

CHAPTER 1

SCOPE OF THE WORK

The development of polymer electrolyte membrane fuel cells (PEMFC)s as efficient and environmentally benign power sources is currently given great attention globally because of increasing environmental concerns and a wish to reduce the dependence of fossil fuels. A fuel cell is an electrochemical device that efficiently converts the chemical energy of a fuel directly into electrical energy. Consequently, fuel cells are attractive alternatives to the internal combustion engine due to their markedly higher efficiency and the emission of water as the only exhaust product.

Nevertheless, fuel cells have yet to reach the major commercial breakthrough. There are a few general problems that need to be overcome before a widespread utilization can become a reality, including a reduction of their cost and an improvement of their performance and durability. Some of these issues could be solved by raising the operating temperature of hydrogen fuel cells, which would improve for instance the electrochemical kinetics, simplify the water management, and allow using low purity reformed hydrogen. The current membrane technology limits the maximum temperature for hydrogen fuel cells to about 80 °C. Hence, the state-of-the-art perfluorinated sulfonic acid membranes need to be replaced in order to attain the industrial goals of high operation temperatures. Aromatic hydrocarbon polymers are well-known for their excellent thermal, mechanical, and chemical stability. Consequently, over the last few years a large number of aromatic polymers have been functionalized with sulfonic acid groups and evaluated as PEMFC membranes.

This doctoral thesis was carried out within the framework of the MISTRA (Swedish Foundation for Strategic Environmental Research) program for fuel cells targeted at high-temperature PEMFC operations for the automotive industry. The aim of the project was to synthesize and study the properties of new sulfonated aromatic proton-conducting polymers for use in PEMFCs at elevated temperature. The molecular structure has a profound impact on the macroscopic membrane properties. A strategy to improve proton conductivity, especially under conditions of low humidity, is the formation of well-connected proton channels. This may be achieved by

concentrating the acid groups to specific chain segments in the polymer and hence promoting the phase separation of ionic and non-ionic domains. In the studies described in this thesis, sulfonic acid groups have either been highly concentrated to specific chain segments in the polymer backbone (Paper I) or separated from the polymer backbone on pendant side chains (Papers II-V). Proton-conducting polymers can be prepared by either the copolymerization of sulfonated and non-sulfonated monomers or by chemical modification of non-sulfonated polymers. As presented in this thesis, both of these methods were employed, i.e., chemical modifications of polysulfones (Papers I-II) and polymerization reactions to yield aromatic homo- and copolymers bearing sulfonated side chains (Papers III-V).

The first part of the thesis consists of a summary that describes the fuel cell and proton-conducting polymers, including a review of alternative structures to promote phase separation. In Chapter 3, synthetic methods for polymer synthesis and chemical modification are described. Chapter 4 presents some special characterization techniques, i.e., small angle X-ray scattering and proton conductivity measurements. Finally, the results and conclusions of the research are described and discussed in Chapter 5.

The second part of the thesis comprises the five journal articles it is based on. In Paper I, the preparation of polysulfones with sulfonic acid groups highly concentrated to specific segments in the polymer backbone is described. These polymers were synthesized by employing a chemical modification via a lithiation – sulfination – oxidation route on polysulfones with varying concentrations and distributions of sulfone links. Paper II presents the concentration of sulfonic acid groups to side chains. Polysulfones carrying various aromatic mono-, di- and trisulfonated side chains were synthesized by employing a variety of combinations of lithiation and nucleophilic aromatic substitution reactions. Paper III reports on the synthesis of a new sulfonated monomer bearing fluorine atoms activated for nucleophilic aromatic substitution reactions. This sulfonated monomer was employed in the preparation of all the polymers, which consequently carried sulfonated side chains, presented in Papers III-V. In Paper IV, the synthesis and properties of aromatic ionomers with different backbone structures is discussed. The preparation and characterization of copolymers, in which the degree of sulfonation was controlled by the addition of non-sulfonated comonomers, is described in Paper V.

CHAPTER 2

INTRODUCTION

2.1 Proton-exchange membrane fuel cells

The first fuel cell was invented already in 1839 by Sir William Groove.[1] In 1933, Sir Francis Bacon presented his hydrogen-oxygen cell with an alkaline electrolyte (AFC). These fuel cells delivered high power densities, but unfortunately degraded rapidly due to the porous nickel cathodes. The first polymer electrolyte fuel cell (PEMFC) was presented by William Grubb in 1955.[2] During the "space race" in the 1950s and 60s, the fuel cells found their first major applications for the production of electricity and water in NASA's Gemini and Apollo programs. During this time, other fuel cell systems were originally conceived: the phosphoric acid fuel cell (PAFC), the molten carbonate fuel cell (MCFC), and the solid oxide fuel cell (SOFC). Unfortunately, the fuel cells from the 1960s suffered from disadvantages such as high cost and short lifetimes,[3] which prevented their commercialization. Today, due to the increasing concerns regarding the environment, an intensive development is directed towards reducing the cost and increasing the durability and performance of PEMFCs for various applications.[4-7]

The fuel cell is an electrochemical device that converts the chemical energy of a fuel directly into electrical energy. In its most basic form, the fuel cell uses oxygen from the air and hydrogen to create water and electricity. Due to the low pollution at the point of use and highly efficient energy conversion, fuel cells are more and more considered as environmentally benign power sources. They are, unlike combustion engines, not limited by the Carnot cycle, and therefore, almost all the chemical energy of the fuel may in theory be converted to electricity.[8]

The polymer electrolyte membrane fuel cell or proton-exchange membrane fuel cell, is the fuel cell system in focus in this thesis. This class of fuel cells currently operates at moderate temperatures and uses a hydrated polymer electrolyte membrane (PEM) to separate the fuel and the oxygen. A single cell consists of porous gas diffusion electrodes, a proton-conducting membrane, anode and cathode catalytic layers, and current collectors with reactant flow fields. The voltage of such a single cell is

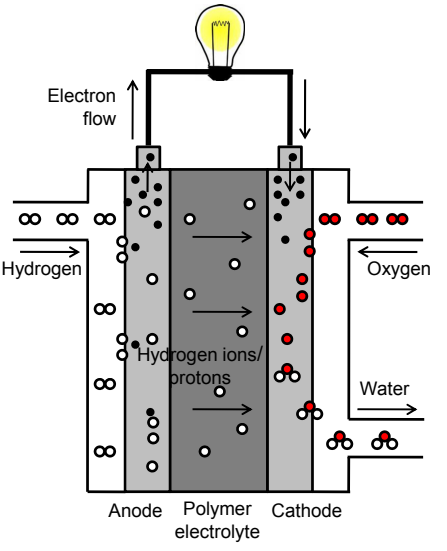

***Figure 2.1**: A schematic representation of a single-cell PEMFC.*

typically around 0.7 V. To yield a higher power output and more elevated voltages, the single cells are incorporated into stacks of cells in series. Cell stacks are further connected in series or parallel, depending on the voltage and current requirements for the specific application. In addition, auxiliaries for thermal and water management and for the compression of gas are required.

Figure 2.1 shows a schematic representation of a single cell. Fuel, commonly hydrogen, is fed to the anode. There, it reacts under the influence of a platinum catalyst and dissociates into protons and electrons (Equation 2.1). The protons are transported through the membrane to the cathode, and the electrons are forced through an external circuit, where the electrical energy is supplied to for instance a light bulb or a car, to the cathode. At the cathode, gaseous oxygen is reduced and combined with protons and electrons to form water (Equation 2.2). The overall cell reaction yields electricity and one mole of water per mole of hydrogen and half a mole of oxygen, according to Equation 2.3.

Anode: $H_2 \rightarrow 2\,H^+ + 2\,e^-$ (2.1)

Cathode: $\frac{1}{2}\,O_2 + 2\,H^+ + 2\,e^- \rightarrow H_2O$ (2.2)

Overall: $H_2 + \frac{1}{2}\,O_2 \rightarrow H_2O$ (2.3)

The PEMFC can alternatively be fed with methanol as fuel to yield carbon dioxide, water, and electricity (Equation 2.4-2.6).

$$\text{Anode:} \quad CH_3OH + H_2O \rightarrow CO_2 + 6\,H^+ + 6\,e^- \qquad (2.4)$$

$$\text{Cathode:} \quad 3/2\,O_2 + 6\,H^+ + 6\,e^- \rightarrow 3\,H_2O \qquad (2.5)$$

$$\text{Overall:} \quad CH_3OH + 3/2\,O_2 \rightarrow CO_2 + 2\,H_2O \qquad (2.6)$$

Unfortunately, the direct methanol fuel cells (DMFC)s present technical problems, including poisoning of the catalyst and diffusion of methanol to the cathode. This problem is commonly called methanol cross-over and results in chemical short circuits leading to lower open circuit voltages. For this reason, the DMFCs have not undergone as rapid development as hydrogen fuel cells, primarily due to the state-of-the-art membranes being very poor methanol barriers.[9]

At temperatures between 50 and 90 °C, the operation of PEMFCs can be problematic due to carbon monoxide poisoning and a low efficiency of the catalyst. Consequently, there is an extensive search for alternative sulfonated polymers that can operate at temperatures higher than 100 °C.[5,10-13] Besides enhanced electrochemical kinetic rates, higher operation temperatures could provide simplified water management and cooling, and the possibility to use reformed hydrogen of lower purity.[5]

2.2 Proton-conducting polymer membranes

The proton-conducting membrane has a key role in the performance of a fuel cell. In addition to high proton conductivity, it should also present a low electronic conductivity and be an efficient barrier for the reactant gases or liquids. During fuel cell operation, the membrane is subjected to a harsh environment including high acidity, free radicals, high temperatures and mechanical stress.[14] Unfortunately, many of the desired properties of a proton-exchange membrane are partly conflicting, and thus, the ionomer has to be a high-performing multifunctional material.

Nafion® and alternative membrane materials

State-of-the-art membranes currently include perfluorosulfonic acid membranes such as Nafion®, which was commercialized by DuPont in 1968.[15] As depicted in Scheme 2.1, Nafion® consists of a Teflon-like fluorinated polymer backbone with fluorinated ether side chains having sulfonic acid end groups. Nafion® is synthesized by copolymerization of perfluorinated vinyl ether comonomers with tetrafluoroethylene (TFE).[16] The number of side chains can be controlled by adjust-

ing the ratio between the comonomers to yield ionomers of various equivalent weights (EW)s. The EW is defined as the mass of polymer per mole of sulfonic acid groups attached to the polymer. A typical EW for Nafion® membrane is 1100. Nafion® membranes show good mechanical properties, high oxidative stability, and high proton conductivities at operation temperatures below 90 °C, provided that the degree of hydration is sufficient.[15,17] Above 90 °C, however, the proton conductivity decreases drastically due to the dehydration of the membrane.[18] In addition, softening of the membrane leads to poor dimensional stability at these temperatures. Another drawback is the high cost.[14] When incorporated in DMFCs, Nafion® membranes have shown elevated methanol permeabilities, thus restricting their use in such fuel cells.[19]

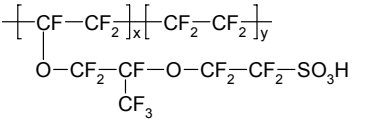

Scheme 2.1*: The chemical structure of Nafion® (x = 1, y = 6-10)*

Due to the above mentioned shortcomings, there is currently an extensive worldwide search for and development of alternative sulfonated and phosphonated polymers for proton-exchange membranes, as thoroughly described in various reviews.[9,10,12,17,20-25] Among these materials, a wide range of sulfonated aromatic hydrocarbon polymers have been evaluated and demonstrated as proton-exchange membranes, including sulfonated poly(arylene ether sulfone)s, poly(arylene ether ketone)s, and polyphenylenes.[9,20,24,25] These polymers have shown high thermal and chemical stabilities, combined with good mechanical properties.

The importance of water

The level of hydration of proton-exchange membranes is very important for the performance of the fuel cell. In the absence of water, the proton conductivity is generally very low. However, at high levels of hydration the mechanical properties are typically compromised because of the high degree of swelling. Consequently, the membrane properties should be tuned so that the water uptake is controlled and kept at a moderate level. The water content in ionomers can be represented either by the water uptake (Equation 2.7) or the number of water molecules per sulfonic acid unit, also referred to as the hydration number and denoted λ (Equation 2.8).

$$\text{Water uptake (\%)} = [(W_{wet} - W_{dry}) / W_{dry})] \cdot 100 \qquad (2.7)$$

$$\lambda = 1000 \cdot [(W_{wet} - W_{dry}) / W_{wet})] / (18 \cdot \text{IEC}) \qquad (2.8)$$

Here, the IEC is the ion-exchange capacity, defined as the number of moles of exchangeable acid protons per gram of dry polymer. The IEC can experimentally be determined by acid-base titration of the sulfonic acid groups. The previously described equivalent weight is the inverse of the IEC according to:

$$EW = 1000 / IEC \qquad (2.9)$$

Ionomers containing ionic groups linked directly to the polymer backbone form ion pairs as a result of strong electrostatic attractive forces. At relatively low temperatures, these ionic pairs or multiplets can aggregate to form clusters.[26] This ionic clustering has been described by Eisenberg *et al.* in various publications on ionomers in general,[26] random ionomers,[27] and sulfonated ionomers.[28] Ionomer membranes normally phase-separate into hydrophobic polymer-rich phase domains and hydrophilic ionic cluster domains during the membrane formation process, as depicted in Figure 2.2a-b. When subjected to water, the ionic clusters absorb water to form a percolating network of nanopores containing water. The absorption of water takes place in two stages. During the first stage, it occurs by solvation of the ions in the membrane (Figure 2.2c),[29] and in the second stage, the percolating network of nanopores is formed during membrane swelling (Figure 2.2d).[9,29]

In these nanopores, the water dissociates the acid units and functions as a proton solvent to facilitate the conduction. The properties of the membrane are also highly dependent on the nature of the hydrophobic phase domain, which plays the important role of maintaining the mechanical strength and dimensional stability of the membrane during fuel cell operation. One of the main challenges in the preparation of proton-conducting membranes is to optimize the molecular structure, and hence,

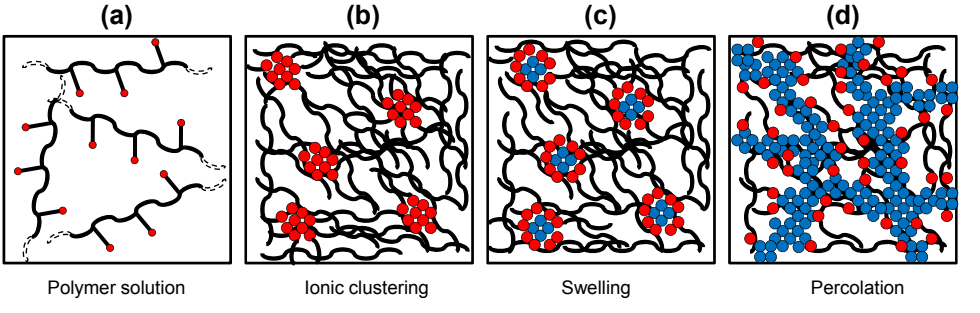

***Figure 2.2**: A schematic representation of the evolution from (a) polymer solution, via (b) ionic clustering during membrane formation, to (c) swelling and (d) percolation upon hydration. The black lines, the red circles, and the blue circles represent polymer chains, sulfonic acid units, and water molecules, respectively.*

balance the combination of hydrophobic and hydrophilic segments in order to obtain the best overall membrane properties.[22,30,31] Aromatic ionomers with sulfonic acid units placed randomly along the polymer backbone have been found to develop quite inefficient networks of nanopores for proton transport, as compared to Nafion®. The aromatic hydrocarbon polymer backbones are less hydrophobic than the backbones in Nafion®, and their sulfonic acid groups are less acidic. In addition, the acid groups are placed on rigid aromatic polymer backbones and hence have a lower mobility and degree of freedom during the membrane formation process.[9] The distance between ionic groups is a contributing factor to water domain features and primarily affect the proton conductivity of the membrane. Consequently, the smaller the distance between the acid groups, the lower the resistive losses associated with proton transport.[32]

The local environment of water in the membrane can be identified from the temperature at which water in the membrane freezes.[33] Non-freezable water interacts strongly with sulfonic acid groups, while freezable water is "free" and not intimately bound to the sulfonic acid groups. Under hydrated conditions, the tightly bound non-freezable water has a critical influence on the depression of the glass transition temperature (T_g), which indirectly affects the proton conductivity.[33,34] The amount of bulk-like freezable water absorbed in the membrane can be estimated from the melting peak in a differential scanning calorimetry thermogram. The amount of freezing water can be calculated by integrating the peak of the melt endotherm and then comparing this value with the heat of fusion of pure ice, i.e., 334 Jg^{-1}.[35] In addition, the state of the water in the ionomers can also be linked to the effect of capillary condensation. The melting point depression of the ionomer water is related to the pore geometry. Assuming a cylindrical geometry of the pores, the pore size radius and distribution in hydrated membranes can be determined by means of nuclear magnetic resonance (NMR) cryoporometry.[36]

Proton conductivity theories

The proton conductivity of a proton-exchange membrane is of great importance since it plays a crucial role in the performance of the fuel cell. An elevated proton conductivity results in a high power density. Proton conduction in a hydrated membrane takes place via two mechanisms; the Grotthuss mechanism and the vehicle mechanism. Both of these mechanisms rely on the fact that the protons lack an electron shell and therefore strongly interact with their environments.[37] In the vehicle mechanism, the protons diffuse with a vehicle, in the form of H_3O^+ (Figure 2.3a). A counter-diffusion of non-protonated H_2O is established to allow a net transport through the membrane. In highly hydrated membranes, as the ones focused on in this thesis, the proton conduction occurs primarily by the vehicle mechanism, particularly at elevated temperatures.[9,32] At lower water contents, the

proton conductivity is more strongly dependent on the mobility of the sulfonic acid groups that take part in the conduction process.[38] In this second case, the Grotthuss mechanism is dominant.

The Grotthuss mechanism is also called the "structure diffusion" since it involves a reorganization of the structure in which the proton diffuses.[39] The structural reorganization involves water molecules, and the proton diffusion occurs as a movement through the water by breaking and forming hydrogen bonds, as depicted in Figure 2.3b. The excess protons exist either as water dimers $H_5O_2^+$, called Zundel ions, or as a hydrated hydronium ions $H_9O_4^+$, called Eigen ions. The rapid transition from a Zundel ion to an Eigen ion and then back to a Zundel ion facilitates the proton diffusion.[40] The Grotthuss mechanism is responsible for the proton conducting character of anhydrous proton-conductors such as imidazoles and benzimidazoles.[41,42]

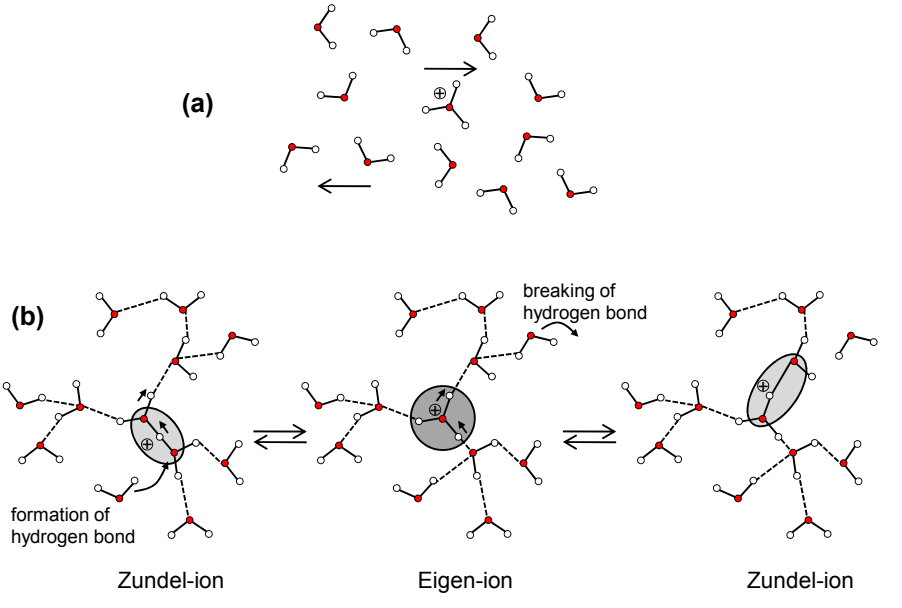

***Figure 2.3**: Proton conductivity mechanisms in water: a) the vehicle mechanism and b) the Grotthuss mechanism.*[40]

Alternative molecular structures for improved phase separation

As discussed earlier, in order to reach a commercial breakthrough for aromatic proton-conducting membranes, it is necessary to improve the proton conductivity, especially under conditions of low humidity and elevated operating temperatures. A key strategy for enhancing the proton conductivity under low humidity is the formation of well-connected proton channels. There are various synthetic methodologies for tailoring molecular structures that promote nanoscale phase separation of ionic and non-ionic domains and consequently enhance the proton conductivity.[25,30] In the following paragraphs, some of these synthetic methodologies are described.

Multiblock copolymers consist of multiple continuous sequences of chemically dissimilar repeating units, as exemplified in Scheme 2.2a. Block copolymers are often able to spontaneously assemble into a wide variety of nanostructures, such as spheres, cylinders, lamellae, and double gyroids.[25] A wide variety of multiblock copolymers have been prepared during the last ten years and among these, the sulfonated-fluorinated poly(arylene ether sulfone) multiblock copolymers have been thoroughly studied.[43-48] Such materials are prepared either by the coupling together of sulfonated and non-sulfonated oligomers with reactive chain ends to yield alternating multiblock copolymers[43,44] or by coupling together oligomers with chain extenders to yield random multiblock copolymers.[45]

Alternative multiblock copolymers, including poly(arylene ether ketone)[49,50] and poly(arylene ether sulfone)-b-polyimide multiblock copolymers,[51] have also been prepared. Highly sulfonated multiblock copolymers have been synthesized by Watanabe *et al.* by a selective post-sulfonation of bulky blocks[52] and by Ueda *et al.* via post-sulfonation of pre-sulfonated hydrophilic blocks.[53] The influence of block length and chemical composition on the properties of proton-conducting sulfonated multiblock copolymers has been studied by McGrath *et al.*[46,54] and Ueda *et al.*[48] Their reports showed that higher proton conductivities were observed for the larger block length materials. In addition, the water uptake was controlled by adjusting the length ratio between the hydrophobic and hydrophilic blocks. Moreover, Ueda *et al.* have compared the properties of random- and alternating multiblock copolymers, indicating higher proton conductivities at reduced relative humidities for the latter.[45]

A second class of copolymers are the star block copolymers, depicted in Scheme 2.2b, which have proven to be interesting due to their unique properties and processing characteristics.[30] There are very few reports of proton-conducting star block copolymers, but those that exist are focused on sulfonated hydrogenated poly(styrene-butadiene) star block copolymers,[55] dendritic-linear copoly(arylene ether)s,[56] and star-shaped sulfonated block copoly(ether ketone)s,[57] where membranes of the latter showed proton conductivity comparable to that of Nafion® at reduced relative humidities.[57]

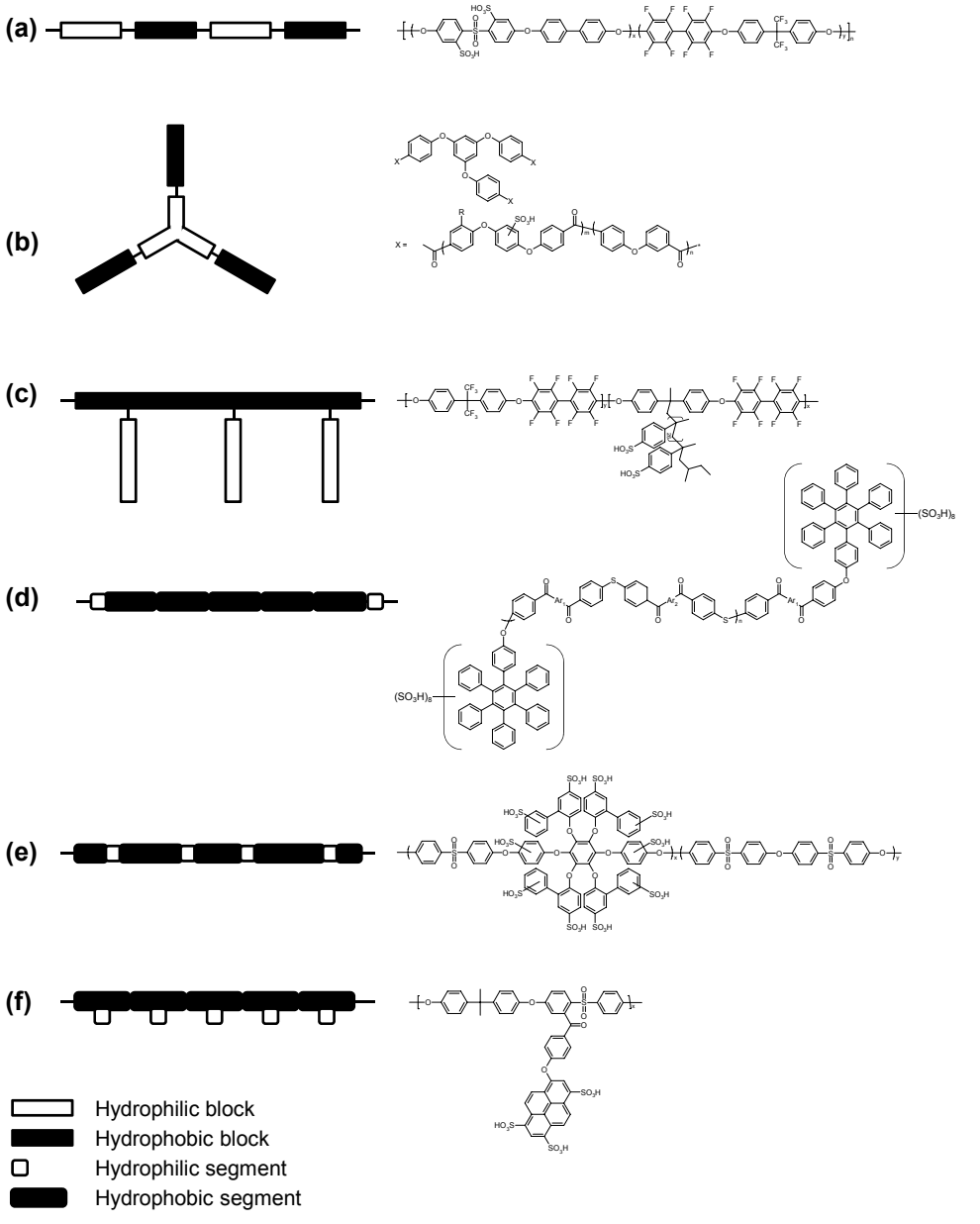

***Scheme 2.2**: Alternative architectures to promote phase separation: a) multiblock copolymers,[43] b) star-shaped copolymers,[57] c) graft copolymers,[61] d) polymers with densely sulfonated end-groups,[64] e) polymers with locally densely sulfonated segments in the polymer backbone,[69] and f) polymers with sulfonated side chains.[76]*

Another interesting class of copolymers are the graft copolymers (Scheme 2.2c), which are well known to exhibit properties differing distinctly from those of their linear counterparts of similar composition.[25] Among the studied proton-conducting graft copolymer membranes, the most extensively investigated are the ones formed by radiation-grafting of styrene onto fluorinated polymer backbones with a subsequent sulfonation of the polystyrene.[58-60] Graft copolymers with ionic polymer grafts attached to a hydrophobic backbone are useful model macromolecules for exploring structure-property relationships in ion-conducting membranes, especially if the length and number density of graft chains can be controlled. The number density and size of ionic aggregates are expected to control the degree of connectivity between ionic domains.[30,61]

An example of controlled graft copolymers has been provided by Holdcroft *et al.*, who reported on the preparation of poly(sodium styrene sulfonic acid) graft chains attached to a hydrophobic polystyrene backbone through a combination of stable free radical polymerization and emulsion polymerization.[62,63] These graft copolymers were found to use their associated water more efficiently to transport protons as compared to random copolymers of polystyrene and polystyrene sulfonic acid.[62] Another example of controlled graft copolymers has been reported by Ding *et al.* and involves the preparation of poly(α-methyl)styrene grafts on fluorinated polymer backbones via anionic polymerization.[61]

Locally and densely sulfonated polymers are capable of a better microphase separation, which enhances the proton conductivity as compared to random copolymers.[25] The preparation of linear and branched ionomers with densely sulfonated (6 to 8 sulfonic acid groups) end-groups (Scheme 2.2d) has been reported by Hay *et al.*[64-66] Nonetheless, it has been found difficult to increase the IEC and proton conductivity of these ionomers due to the sulfonated groups being located only at the chain ends. Consequently, an alternative route involves the incorporation of densely sulfonated groups randomly distributed in the polymer backbone, as can be seen in Scheme 2.2e. Hay *et al.*[67] and Ueda *et al.*[68,69] have reported on the preparation of ionomers containing clusters of 6 to 12 sulfonic acid groups randomly distributed along the polymer backbone.

Moreover, Colquhoun *et al.* have introduced a new concept with regards to high-temperature, swelling-resistant membrane: microblock ionomers.[70] These ionomers displayed an organized sequence distribution with fully defined ionic segments, with single, double, or quadruple sulfonic acid groups, separated by fully defined non-ionic spacer segments. These strictly alternating ionomers exhibited very different properties and morphologies compared to their randomly substituted ionomer analogues. By increasing the non-ionic spacer length, while maintaining a constant IEC through an augmentation of the degree of sulfonation in the ionic segment, the

degree of nanophase separation was shown to increase. Significantly higher onset temperature for uncontrolled swelling in water was observed.[70] Similar trends have been reported by McGrath *et al.* for sulfonated aromatic polymers with varying sequence lengths, indicating larger ionic domains in alternating copolymers as compared to in random copolymers.[71]

One promising way to enhance the phase separation is to distinctly separate the hydrophilic sulfonic acid groups from the polymer backbone by locating the sulfonic acid groups on side chains as depicted in Scheme 2.2f. The use of chemical modifications to graft sulfonated side chains onto polysulfone backbones has been thoroughly investigated in our research group.[72] Alternatively, side chains can be incorporated onto the polymer backbone by polycondensation reactions with monomers bearing pendant sulfonic acid groups. By employing these two methods, several poly(arylene ether sulfone)s with sulfonated aromatic,[73-77] aliphatic,[78] and aromatic/aliphatic[79] side chains have been prepared and investigated. Furthermore, alternative ionomer backbones have been modified with side chains bearing sulfonic acid groups, such as poly(arylene ether ketone)s,[80] polybenzimidazoles,[81] and polyimides.[82,83] Watanabe *et al.* recently reported on the preparation of poly(arylene ether)s containing pendant sulfonated fluorenyl groups. These so-called superacid groups are similar to the side chains of Nafion®.[84]

Although advanced copolymers, such as sulfonated multiblock copolymers, have shown higher proton conductivities under reduced relative humidity (RH) in comparison with homopolymers and random copolymers,[54,71] appropriately designed polymers of the latter types are still highly interesting for fuel cell applications. The reason is the larger number of available synthetic routes and the ease of preparation as opposed to usually very complex methods required for block copolymers. Consequently, the decision was taken to develop synthetic methods for the preparation of sulfonated homopolymers and random copolymers bearing locally densely sulfonated segments in the polymer backbone or on the side chains. These materials were synthesized by chemical modification of polysulfones or by polycondensation employing sulfonated monomers. The properties of these materials were studied with the aim to distinguish structural features that provide durable high performance membranes for high-temperature PEMFC applications.

CHAPTER 3

POLYMER SYNTHESIS AND CHEMICAL MODIFICATION

3.1 Characteristics of polysulfones

Poly(arylene ether sulfone)s are a class of engineering thermoplastics displaying excellent properties such as a high T_g and a superior thermooxidative stability.[85,86] Two main synthetic routes to poly(arylene ether sulfone)s have been reported: the Friedel-Craft process, which is an electrophilic aromatic substitution, and the polycondensation reaction, which is a nucleophilic substitution of activated aromatic dihalides. A variety of common poly(arylene ether sulfone)s is commercially available, including polyethersulfone (PES), polysulfone-6F, polyphenylsulfone (PPSU) and polysulfone (PSU). The molecular structure of the latter is shown in Scheme 3.1 and will be further discussed in the following paragraphs.

PSUs are commercially available from Solvay Advanced Polymers and BASF, under the trademarks Udel® and Ultrason S, respectively. They are completely amorphous, have a T_g of 190 °C, and decompose at 500 °C under an inert atmosphere. These PSUs are useful engineering plastics since they can be easily molded and processed, and are employed for high-performance applications such as aircraft components, microwave cookware, and pacemakers.[86]

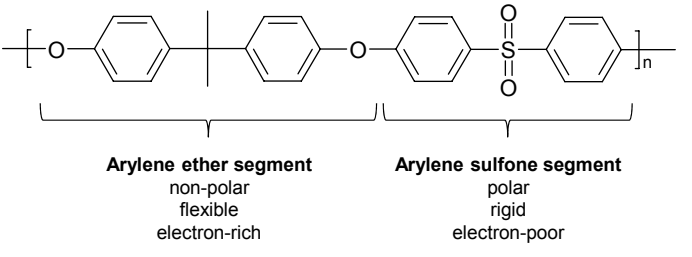

***Scheme 3.1**: Molecular characteristics of the PSU backbone.*

The high T_g of the PSUs depends on chain rigidity and polarity. The polar arylene sulfone segment is extremely rigid because of the phenyl groups and the presence of the inductive polar sulfone groups. The elevated polarity of the sulfone groups leads to an electron-withdrawing effect, which delocalizes the π-electrons from the aromatic rings.[86] The resulting double-bond character of the C-SO_2-C link restricts rotation and consequently enhances chain rigidity.[85] In contrast, the ether bonds and the non-polar 2-isopropylidene links have a comparatively low rotational barrier, which provides flexibility in the arylene ether segment. The valence angles between C-SO_2-C and C-O-C are 105 ° and 124 °C, respectively, and the difference between the two reduces the packing density in the unit cell. As a consequence, most PSUs are fully amorphous, despite their symmetrical chains.[85]

PSUs are soluble in organic solvents such as *N,N*-dimethylformamide, dichloromethane, and tetrahydrofuran (THF) and are hence interesting for carrying out chemical modifications. However, due to their chemical stability, very few options are available for efficient chemical modifications. As shown in Scheme 3.1, two repeating segments can be identified. In the arylene ether segment, the ether groups and the 2-isopropylidene groups are electron donors to the neighboring phenylene rings. Consequently, these electron-rich phenylene rings can be modified by electrophilic substitution reactions, such as direct sulfonation with for instance fuming sulfuric acid, as will be described in the next paragraph. In contrast, the electron-withdrawing effect of the sulfone groups in arylene sulfone segments is strong enough to give an acidic character to the *ortho*-to-sulfone hydrogens. This offers the possibility to chemically modify the PSUs by lithiation reactions as will be described later.

3.2 Direct sulfonation of polysulfones

The introduction of sulfonic acid groups to the polymer backbones of commercially available PSUs is often performed by post-modification using strong acids.[87,88] Direct sulfonation of PSUs was first performed by Noshay *et al.* with a sulfur trioxide-triethyl phosphate complex as the sulfonating agent.[89] Other sulfonating agents exist, such as fuming sulfuric acid,[90] SO_3,[91] chlorosulfonic acid,[92] and trimethylsilyl chlorosulfonate.[93]

As previously discussed, the phenyl rings in the arylene ether segment are rich in electrons due to the electron-donating effect of the ether links. Moreover, these positions are activated for electrophilic substitution. The ease of sulfonation also means that the polymers may be activated for desulfonation under acidic aqueous conditions during fuel cell operation, especially at temperatures exceeding 100 °C.[94,95] Unfortunately, due to the required conditions being harsh electrophilic

sulfonations often lead to issues such as side reactions causing polymer degradation or crosslinking.[87] Another complication for the randomly sulfonated PSUs is an unsatisfactory swelling behavior. These materials usually lose their mechanical stability when a certain critical degree of sulfonation, or temperature, is exceeded under immersed conditions.[9] For example, directly sulfonated PSUs with a degree of sulfonation of 80% have been found to be water-soluble at room temperature, thus restricting their use as membranes in fuel cells.[96]

3.3 Lithiation of polysulfones

Lithiation followed by electrophilic substitution is a powerful method for modifying PSUs. The first study on the lithiation of PSUs was published by Breihoffer *et al.* in 1986,[97] and dealt with the carboxylation of PSU by lithiation in THF at room temperature, followed by the addition of carbon dioxide. The lithiated PSU precipitated at a relatively low degree of modification, which was explained by the interaction between lithium sites on the polymer backbone. Additionally, an uneven carboxylation substitution among polymer molecules was reported.

The mechanism behind the lithiation of PSUs was first presented in 1988, by Guiver *et al.*[98] In that study, lithiated PSU was reacted with deuterium oxide or iodomethane in order to identify the reactive sites on the PSU backbone through proton NMR (^{1}H NMR) spectroscopy. The spectra confirmed that the site of lithiation was at the *ortho*-to-sulfone position, and that the degree of lithiation (DL), i.e., the number of lithiated carbons per repeating unit, could be conveniently controlled by the amount of *n*-butyllithium (*n*-BuLi) added up to DL = 2. In addition, ^{1}H NMR spectra indicated that the reaction was rapid and nearly quantitative, and required no excess of reagent or catalyst. Guiver *et al.* reported that the temperature had to be maintained in the temperature range between -10 °C to -78 °C in order to prevent intramolecular rearrangements, which might lead to premature precipitation.

As previously discussed, the electron-withdrawing effect of the sulfone links in the PSU is strong enough to give an acidic character to the *ortho*-to-sulfone hydrogens. This enables their replacement using strong organic bases such as *n*-BuLi. In addition, the lone electron pairs of the sulfone groups stabilize the lithium cations in the form of complexes, as can be seen in Scheme 3.2.

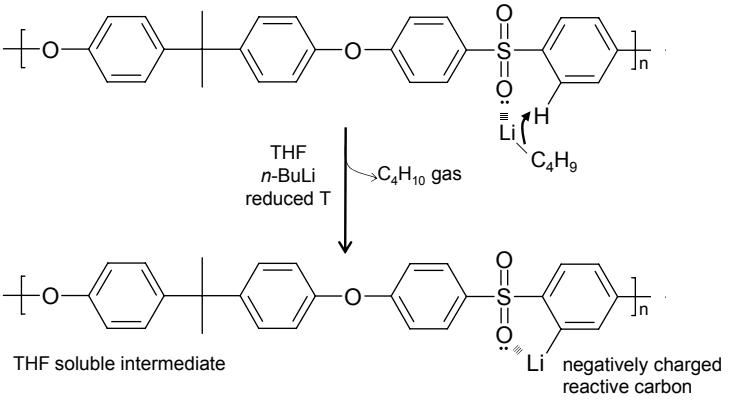

***Scheme 3.2**: Direct lithiation of the PSU backbone using n-BuLi*

After lithiation, the PSU backbone is activated for reaction with various electrophilic reagents. An advantage is the vast number of commercially available electrophiles that allow for a variety of modifications to be carried out.[72] Many of these electrophiles have a potential for crosslinking, and must thus be added quickly, in excess, and at an optimum temperature to efficiently quench the reactive carbanions. In a patent, Guiver *et al.* presented a wide variety of functional groups that can be attached to the PSU backbone by using simple electrophiles.[99]

Lithiation chemistry also opens possibilities to prepare sulfonated PSUs in which the sulfonic acid groups are located on deactivated electron-poor positions of the backbone, in contrast to the direct sulfonation methods previously discussed. Consequently, Kerres *et al.* prepared backbone-sulfonated PSUs by reacting lithiated PSU with sulfur dioxide. The resulting sulfinate groups were subsequently converted to sulfonate groups by various oxidizing agents including hydrogen peroxide, sodium hypochlorite, and potassium permanganate.[100] The sulfinated intermediates were, as discussed in a subsequent publication, partly oxidized and the mixed sulfinated/sulfonated PSUs were crosslinked by adding diiodoalkanes.[101] PSUs bearing sulfoalkylated side chains were prepared by Karlsson *et al.* by grafting sulfinated PSUs with a sulfoalkyl sodium salt.[78] In addition, PSUs bearing sulfonated aromatic side chains[73-76] and phosphonated side chains[102-104] have been prepared in our group, by means of lithiation chemistry.

3.4 Nucleophilic aromatic substitution reactions

Nucleophilic aromatic substitution, S_NAr, is the most commonly employed route to prepare high molecular weight linear poly(arylene ether)s for commercial purposes. The ether links are formed by polycondensation reactions between bisphenols and activated dihalides[105,106] according to:

XAr′X + MOAr′′OM → -Ar′OAr′′O- + 2MX

or by difunctional monomers containing both halide and phenol functionalities:

XAr′OM → -Ar′O- + MX

Here, X is a halogen and M is an alkali metal ion. The reaction rates are dependent on the basicity of the bisphenol salt and on the electron-withdrawing effect in the dihalide.[107] In the preparation of poly(arylene ether sulfone)s, bis-phenolates are generally reacted with bis(4-chlorophenyl)sulfone (dichlorodiphenyl sulfone, DCDPS) as depicted in Scheme 3.3. The strong electron-withdrawing effect of the sulfone link increases the reactivity of the aromatic chloride in order for chlorine to be easily displaced from the aromatic ring. Occasionally, the more reactive difluorodiphenyl sulfone is used.

In the preparation of poly(arylene ether ketone)s, bis-phenolates are generally used in their alkali metal salt form or alternatively, as bis-trimethylsilylated bisphenol.[108,109] Due to the lower electron-withdrawing effect of the ketone link compared to the sulfone link, fluorinated aromatic monomers, such as 4,4'-difluorobenzophenone, are used in order to obtain high molecular weight polymers.

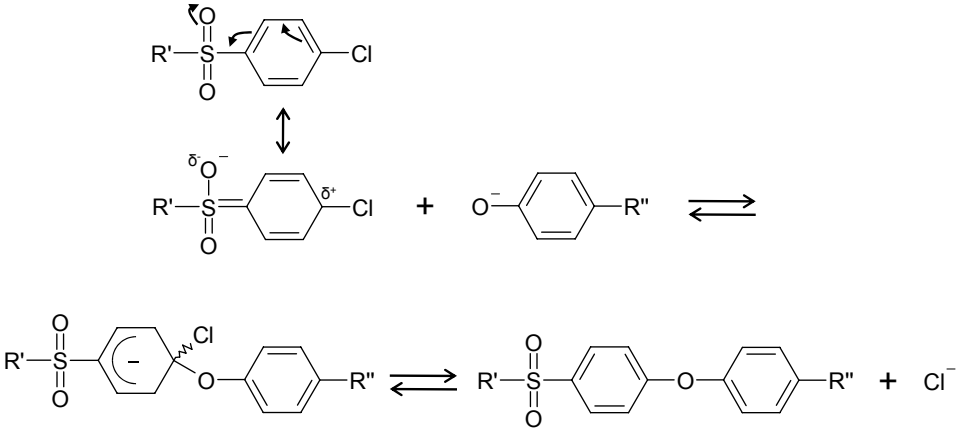

Scheme 3.3*: The mechanism for preparing poly(arylene ether sulfone)s by nucleophilic aromatic substitution.*

The nucleophilic aromatic substitution reactions are step-growth polymerizations governed by the Carother's equation. Consequently, a high degree of polymerization is only achieved at high monomer conversion. The nucleophilic aromatic substitution reactions are thus very susceptible to monomer impurities and are dependent on stoichiometry to yield high molecular weight polymers. The monomers thus have to be thoroughly purified, commonly by recrystallization, prior to use.

The solvent plays an important role in the polymerization reactions. Besides enhancing the rates of substitution, it must also keep the reactants and the resulting polymers in solution. Only a limited range of suitable solvents with necessary temperature performance and solvating properties is known. In the preparation of poly(arylene ether sulfone)s, dipolar aprotic solvents such as dimethylsulfoxide (DMSO), *N,N*-dimethylacetamide (DMAc), *N*-methyl pyrrolidone (NMP), and sulfolane are used.[105] Poly(ether sulfone)s based on 4,4'-sulfonyldiphenol (bisphenol S) rather than 4,4'-isopropylidenediphenol (bisphenol A) require higher reaction temperatures due to a reduced solubility and a reduced nucleophilicity of the phenolate ions. For this purpose, solvents with higher boiling points and of higher thermal stability are required. Poly(ether ketone)s are semicrystalline and will therefore not remain in solution during polymerization unless elevated temperatures are employed. With diphenyl sulfone (DPS) as the solvent, these polymerization reactions can be carried out in the temperature range close to the melting point of the polymers, i.e., 334 °C for poly(ether ether ketone) (PEEK).[110]

The alkali ion as well as the manner in which the bis-phenolate salts are produced is also of importance for the polymerization. For chloroaromatic monomers, the potassium salt is generally necessary in order to yield an acceptable reaction rate. For the fluoroaromatic monomers however, the sodium salt is typically sufficient. Nevertheless, the reaction rates tend to be slow and may lead to side-reactions and to the formation of gels. In practice, either the potassium salt or a mixture of potassium and sodium salts is employed. An alternative method has been reported by Kricheldorf *et al.*, in which the trimethylsilyl derivates of the phenol is used with cesium fluoride as a catalyst. In this case, the fluoride ion converts the trimethyl siloxy groups into a phenolate ion, which in turn attacks the activated fluorine-carbon bond in the activated difluoro monomer.[108,109] The alkali-phenolates may be prepared either by a pre-reaction of the bisphenol with potassium hydroxide, or *in situ*, by employing a small excess of potassium carbonate in the mixture of activated difluoride and bisphenol. In the preparation of polysulfones, the bisphenol is generally pre-reacted with a strong base in DMSO and an azeotroping solvent, such as toluene. The reaction mixture is then added to a second reactor containing the DCDPS together with more azeotroping solvent for the removal of water.

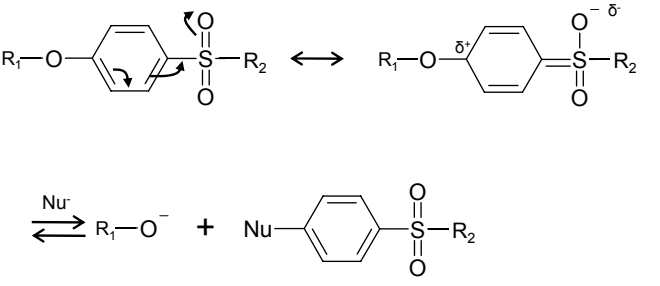

Scheme 3.4*: The mechanism for transetherification of polysulfones.*

The alkali metal salts also play an important role in the process of transetherification, to which the polysulfones and PEEKs are susceptible. The ether linkages in polysulfones and PEEK are electron-deficient due to the mesomeric effect from the electronegative linking groups, as illustrated in Scheme 3.4. Consequently, these ether links are susceptible to cleavage by nucleophiles, such as hydroxide and fluoride anions.

The degree of transetherification has been shown to be related to the base used in the polymerization reaction. In a report by Colquhoun *et al.*, it was shown that the degree of transetherification was increased by the introduction of small amounts of potassium salt, as opposed to the sodium salt; a phenomenon explained by the higher solubility of the potassium salt, which increases the concentration of nucleophilic fluoride anions.[111] The role of the anion in nucleophilic cleavage and transetherification reactions at high temperatures has also been studied by Carlier *et al.*[112]

3.5 Random copolymerization

An alternative route to obtain sulfonated aromatic polymers is to first prepare sulfonated monomers and then synthesize the polymers using suitable comonomers in nucleophilic aromatic substitution reactions. Through this route, the hydrophilicity of the copolymers can be readily controlled by adjusting the molar ratios of sulfonated to non-sulfonated monomers. Moreover, it becomes possible to prepare pre-sulfonated monomers with the sulfonic acid groups placed on deactivated sites, which gives polymers that are less prone to desulfonation as compared to counterparts sulfonated by electrophilic substitution reactions.[95]

Commonly used disulfonated monomers are depicted in Scheme 3.5.

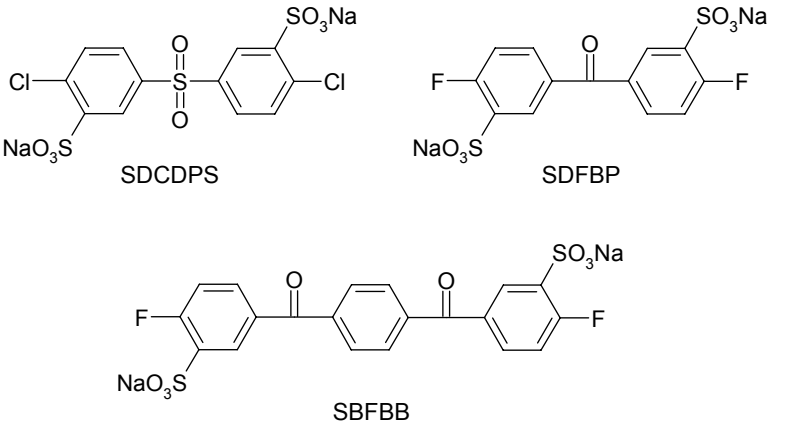

Scheme 3.5*: Molecular structures of disodium 3,3-disulfonate-4,4'-dichlorodiphenyl sulfone (SDCDPS), disodium 3,3-disulfonate-4,4'-difluorobenzophenone (SDFBP), and 1,4-bis(3-sodium sulfonate-4-fluorobenzoyl)benzene (SBFBB).*

A wide variety of random poly(arylene ether sulfone) copolymers based on the disodium 3,3'-disulfonate-4,4'-dichlorodiphenyl sulfone (SDCDPS) have been prepared, with various non-sulfonated dihalogenated monomers and hydrophobic bisphenol.[31,113-119] As depicted in Scheme 3.6a, the concentration of sulfonic acid groups can be high, which has been found to give rise to elevated proton conductivities. The influence of the hydrophobic bisphenol structure on the properties of the copolymers has been discussed by McGrath *et al.*[115] and Watanabe *et al.*[31] Sulfonated poly(ether ether ketone) (sPEEK) copolymers with a controlled degree of sulfonation have been prepared using 3,3-disulfonate-4,4'-difluorobenzophenone (SDFBP) as comonomers.[120-122] By incorporating various bisphenols, a variety of sPEEK copolymers can be synthesized, as can be seen in Scheme 3.6b. The copolymer structure can be further modified by employing various non-sulfonated dihalogenated comonomers, resulting in for example sulfonated poly(benzoxazole ether ketone) copolymers,[123] or sulfonated poly(phthalazinone ether ketone nitrile) copolymers.[124] By using 1,4-bis(3-sodium sulfonate-4-fluorobenzoyl)benzene (SBFBB), with an additional ketone link, as the sulfonated monomer, sulfonated poly(arylene ether ether ketone ketone) copolymers can be synthesized, according to Scheme 3.6c.[125]

Guiver *et al.* have in various publications described the preparation of completely aromatic sulfonated copolymers containing polar nitrile groups, which have exhibited a reduced water uptake due to an increase in inter-chain molecular forces.[124,126-128] Additionally, Guiver *et al.* have prepared sulfonated copolymers bearing naphthalene moieties incorporated in the polymer backbone in structurally

different ways, as depicted in Scheme 3.6d.[122,126,128,129] Random copolymers with pendant sulfonated side chains have furthermore been synthesized, according to Scheme 3.6e. Watanabe *et al.* have described the preparation of polyimide copolymers bearing sulfoalkyl side chains and showing an improved thermal stability due the presence of triazole groups.[82,83] The preparation of poly(arylene ether) copolymers bearing sulfoalkyl side chains has been reported by Jiang *et al.*[79]

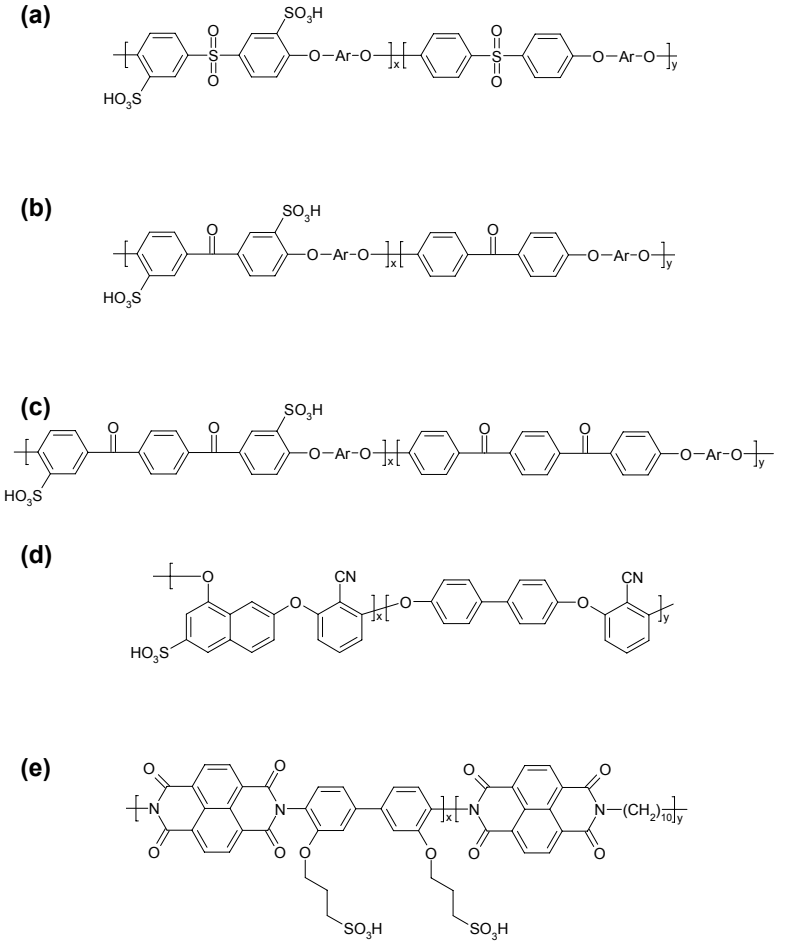

Scheme 3.6*: Examples of statistical copolymers: (a) sulfonated copoly(arylene ether sulfone);*[31,113-116,118] *(b) and (c) sulfonated copoly(arylene ether ketone);*[120-122,125] *(d) sulfonated copoly(arylene ether nitrile);*[126] *and (e) copolyimide with pendant sulfoalkyl side chains.*[83]

CHAPTER 4

SPECIAL CHARACTERIZATION TECHNIQUES

4.1 Small angle X-ray scattering (SAXS)

Small angle X-ray scattering (SAXS) is a technique where elastic scattering of X-rays is recorded at very low angles, typically 0.1 to 10 °. As shown in Figure 4.1, an X-ray generator provides a monochromatic X-ray beam, which is directed towards the sample. Most of the X-rays pass through the sample without interaction and form a primary beam. However, due to inhomogenities in the sample, some X-rays are elastically scattered, creating an angular distribution of the X-ray beams reaching the detector. This angular distribution contains information about the shape and size of the macromolecules in the sample, as well as characteristic separation lengths between ordered structures.

The detector is typically a two-dimensional flat detector located behind the sample in a direction perpendicular to the primary beam, as shown in Figure 4.1. The SAXS pattern is generally represented as scattered intensity as a function of the magnitude of the scattering vector, q

$$q = (4\pi / \lambda) \cdot \sin\theta \qquad (4.1)$$

where 2θ is the scattering angle and λ is the wavelength of the X-rays. For samples with ordered structures, the characteristic separation length d, also known as the Bragg spacing, can be calculated according to

$$d = 2\pi / q \qquad (4.2)$$

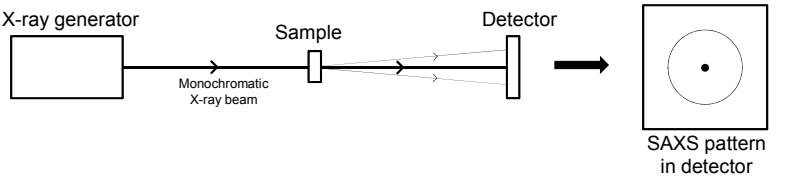

Figure 4.1*: A schematic drawing of the SAXS instrument and the signals detected.*

SAXS is a commonly used method to study the morphology of polyelectrolyte membranes. The morphology of the membranes is observed in terms of the position, i.e., the *q* value, and width of the so-called ionomer peak.[130] Ionomers were first studied by SAXS in the 1960s, during which the first observation of SAXS peaks, attributed to ion segregation in the hydrophobic polymer matrix, were reported by Longworth *et al.*,[131] followed by a deeper investigation by Eisenberg.[26] Various models have been proposed to interpret the SAXS observations, and they can generally be classified into intraparticle models,[132] and interparticle models.[133-135] The intraparticle models attribute the ionomer peak to the interference within the ionic clusters implying that the scattering maximum is related to the internal structure of the clusters. The interparticle models, on the other hand, attribute the ionomer peak to the interference between different ionic clusters which indicate that the Bragg spacing (Equation 4.2), is the center to center distance between two clusters. The origin of the ionomer peak is still not fully resolved, but the interparticle models are now commonly accepted.

SAXS studies on proton-conducting ionomers were first reported in the 1980s. Based on SAXS studies on water swollen Nafion® membranes, Gierke *et al.* proposed a model of swollen spherical aggregates connected by narrow channels.[136] Additionally, they discovered that the cluster size was smaller than the characteristic separation length deduced from the ionomer peak position. Since then, the morphology of Nafion® swelled with water as well as under dry conditions has been thoroughly studied by SAXS.[15,137] During the last ten years, alternative proton-conducting membranes have been studied. The influence of cast solvent effects[138] and the degree of sulfonation[139] on the morphology of sPEEK, along with differences in hydration behavior[140] based on the morphology in sPSU, have been explored by SAXS. Moreover, the effect of crystallinity on the morphology of backbone-sulfonated poly(1,4-phenylene sulfide) has recently been investigated with the technique.[141] However, other alternative sulfonated proton-exchange membranes have received much less attention.[142,143]

4.2 Proton conductivity measurements

The proton conductivity of polymer electrolytes is generally measured by electrochemical impedance spectroscopy (EIS). A sinusoidal voltage (U*) at a fixed frequency (ω) is applied to the sample and a sinusoidal current (I*) with the same frequency, but with a phase shift (φ), is monitored. The phase shift originates from the reorientation of the ionic and dipolar groups in the sample when subjected to the electric field. The more difficult it is for the dipoles to reorient, the larger the

phase shift. The complex impedance is given by the relationship between the voltage and the current according to

$$Z^* = U^* / I^* \qquad (4.3)$$

By measuring the impedance at various frequencies and temperatures, information about the segmental mobility and the proton conductivity of the ionomer can be obtained. As presented in Figure 4.2, impedance is generally plotted in the complex plane (-Z'' vs. Z') in a so called Cole-Cole or Nyquist plot. The frequency independent impedance (dc resistance), also called the bulk resistance, is denoted Z, and is taken as the real value where –Z'' has its minimum, as indicated in Figure 4.2.

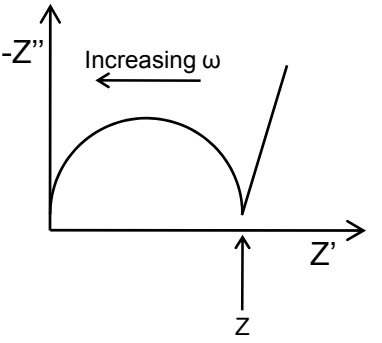

***Figure 4.2**: A Cole-Cole or Nyquist impedance plot.*

The dc-conductivity, σ, is related to the bulk resistance according to

$$\sigma = t / (A \cdot Z) \qquad (4.4)$$

where t is the thickness and A is the cross-section of the sample.

The cell geometry and electrode configuration has been found to play an important role during impedance measurements.[144] Different electrode geometries have been investigated, among which the two- and four-electrode configurations are commonly used. The two-electrode cells have a less complicated configuration, and may hence involve fewer stray effects in the impedance spectra. However, it has been reported that interfacial impedance dominates the response at frequencies up to 100 kHz in the two-electrode configuration, and a four-electrode cell has thus been proposed as a means to avoid these problems.[145] In other studies, the two-electrode cells have shown reliable results, provided they are obtained at higher frequencies.[146,147]

CHAPTER 5

THESIS WORK

The focus of this thesis was to establish structure-property relationships of sulfonated proton-conducting polymers. To this end, several ionomers were synthesized and characterized with respect to their nanoscale structure and key membrane properties. As mentioned in the introduction, ionomers with sulfonic acid groups randomly grafted directly onto the hydrophobic polymer backbone have shown an excessive water uptake and the loss of mechanical integrity when a certain degree of sulfonation or a certain temperature is exceeded. The properties of these ionomers can be considerably improved by concentrating the sulfonic acid groups to specific chain segments in the polymer, thus enhancing phase separation.

As a first step in this direction, the sulfonic acid groups were highly concentrated to specific segments in the polymer backbone by employing a lithiation – sulfination – oxidation route on PSUs with varying concentrations and distributions of sulfone links (Paper I). As a second approach, the sulfonic acid groups were concentrated to side chains. PSUs carrying aromatic mono-, di- and trisulfonated side chains were synthesized by employing combinations of lithiation and nucleophilic aromatic substitution reactions (Paper II). PSUs with sulfobenzoyl side chains were found to have almost completely suppressed ionic clustering, which was partly explained by the proximity between the sulfonic acid groups and the polymer backbone.

Based on these findings, the idea was to investigate the influence of the backbone structure on the properties of aromatic ionomers with pendant sulfobenzoyl side chains (Papers III-V). The ionomers described in these three papers were prepared by nucleophilic aromatic substitution reactions, polycondensations, which offer a large variety in sulfonated- and non-sulfonated monomers. For this purpose, a new monomer bearing fluorine atoms activated for nucleophilic aromatic substitution reactions was obtained by using a lithiation approach. The preparation of this monomer, 2,6-difluoro-2'-sulfobenzophenone (DFSBP), and the consequent polymerizations, resulting in two high molecular weight polymers with sulfobenzoyl side chains, are reported on in Paper III.

Paper IV presents the preparation of aromatic ionomers with different backbone structures by polycondensations of DFSBP, one dithiol and various diols. As expected from their high IEC values, these ionomers had too high water uptake levels for practical use as proton-exchange membranes. The ionomer bearing naphthyl moieties in the backbone was found to have a high intrinsic viscosity, good thermal properties, and an adequate level of proton conductivity, for which reason it was chosen for further investigation. Consequently, copolymers with backbones bearing naphthyl moieties and with pendant sulfobenzoyl side chains were synthesized via polycondensations using two non-sulfonated comonomers for variation of the IEC, and an expected control of the water uptake (Paper V). Scheme 5.1 shows a graphical illustration of the ionomers included in this thesis.

As indicated in Scheme 5.1, two separate synthetic pathways were employed to prepare the ionomers reported on in this thesis: chemical modifications via lithiation and polycondensation reactions. The following paragraphs offer a description of the laboratory setup and the practical considerations regarding these two methods.

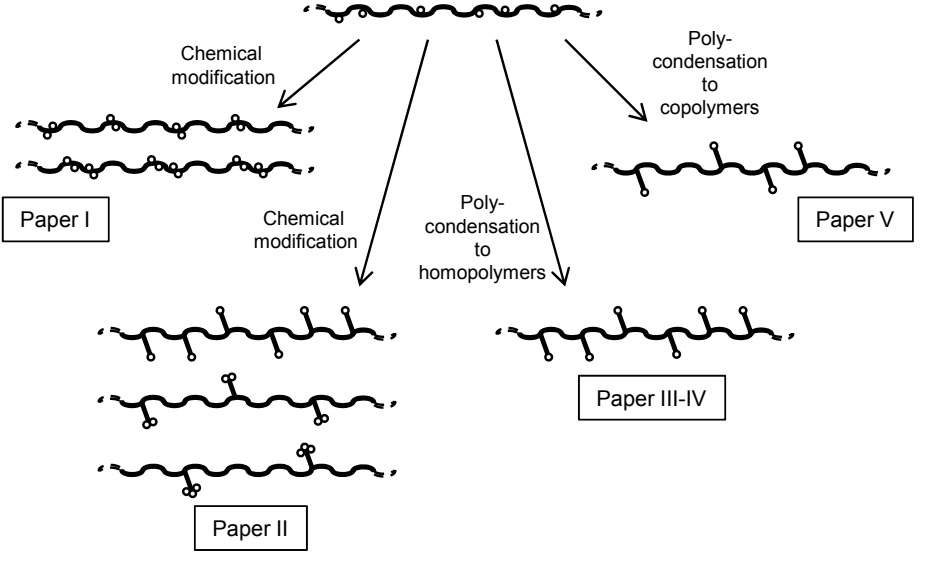

Scheme 5.1*: A graphical illustration showing the evolution from an ionomer with the ionic sites (white circles) randomly placed on the backbone (top) to an ionomer with the ionic sites concentrated to specific segments in the backbone (Paper I), the ionic sites concentrated to side chains by chemical modification of PSUs (Paper II), and homopolymers (Papers III-IV) as well as copolymers (Paper V) prepared by polycondensations.*

Chemical modification via lithiation

A chemical modification via lithiation of PSUs was employed to obtain the ionomers presented in Papers I-II. In addition, the sulfonated monomer used for the preparation of the ionomers discussed in Papers III-V was prepared by lithiation chemistry. The laboratory setup for the lithiation reactions is shown in Figure 5.1. Due to the extremely high reactivity of *n*-BuLi with water, it was of utmost importance to use thoroughly dried glass equipment, solvents, and chemical reactants. In a typical procedure, the thoroughly dried polymer was dissolved in THF, previously dried with molecular sieves, in an air-tight round-bottomed flask connected to an argon gas supply. Thereafter, the polymer solution was cooled by means of dry ice in an isopropanol bath. At -40 °C, the solution was carefully degassed, by alternating vacuum and argon supply, followed by cooling to -70 °C under a blanket of argon. The *n*-BuLi solution was then added dropwise through the septum from a gas-tight syringe, and the obtained solution was thereafter left for 30 minutes at -70 °C, to complete the lithiation process, after which the electrophile was quickly added. The electrophile can be added either as a gas, as shown in Figure 5.1, as a liquid through the septum from a gas-tight syringe, or as a powder from a glass flask. After a reaction time ranging from a few minutes to 45 minutes, the product was purified and dried.

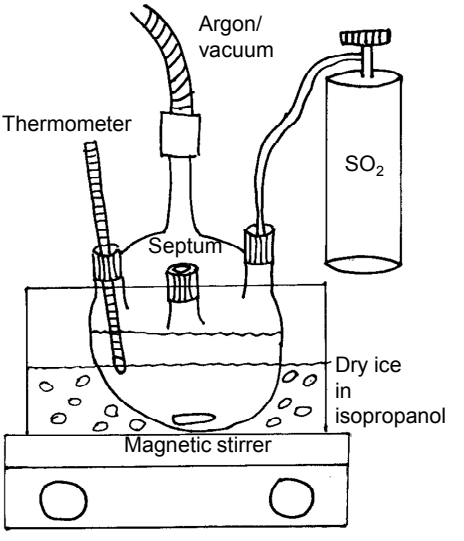

Figure 5.1*: A schematic representation of the equipment used for the lithiation reactions.*

Polycondensation

Polycondensation reactions were employed to prepare the ionomers presented in Papers III-V. The laboratory setup for the polycondensation reactions is shown in Figure 5.2. To yield high molecular weight polymers, the monomers needed to be charged to the reactor in equimolar amounts and it was therefore important to carefully weigh the monomers with an analytical balance. In a typical procedure, the dried monomers and the potassium carbonate salt were carefully weighed in glass beakers, after which they were added to a round-bottomed flask. The polymerization solvent, DMAc, was charged to the beakers to dissolve the remaining monomer, and was subsequently transferred into the round-bottomed flask. Toluene, typically in an amount equal to DMAc, was charged to the reaction mixture and the magnetic stirring was started along with the nitrogen gas flow. Before heating the reaction mixture to 160 °C, a cooling water flow was switched on and the Dean-Stark trap was filled with toluene, thus ensuring a constant volume of toluene in the reactor. During the dehydration step at 160 °C, the water that was formed was removed from the reactor by azeotropic distillation with toluene. After four hours, the Dean-Stark trap was emptied and the toluene was allowed to boil off. Finally, the reaction temperature was raised to 175 °C and the polymerization proceeded until a high viscosity was reached.

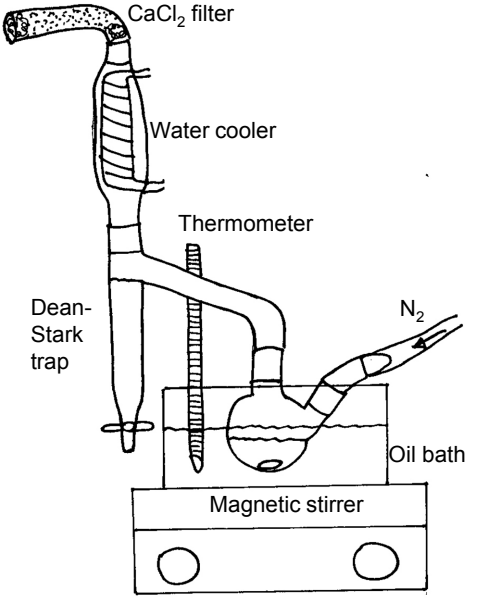

***Figure 5.2**: A schematic representation of the equipment used for the polycondensations reactions.*

5.1 Polysulfones carrying highly sulfonated segments (Paper I)

Paper I reports on the preparation and investigation of a series of highly sulfonated PSUs with the sulfonic acid groups placed in deactivated positions on the polymer backbone (see Scheme 5.2). In a first step, PSUs with varying distributions of sulfone bridges in the backbone were synthesized by polycondensations. Bisphenols were chosen as comonomers in order to vary the chain length in-between the sulfonated segments while maintaining the same structural units in the hydrophobic parts of the polymers. The polymers were sulfonated via lithiation, followed by reaction with sulfur dioxide and finally oxidation of the resulting sulfinates. This procedure rendered it possible to introduce two sulfonic acid units on electron-deficient aryl rings in *ortho*-positions to each sulfone bridge of the PSUs. The fully sulfonated PSUs had IECs of 3.3-4.1 meq./g and were water soluble. Obviously, the water solubility prevented the preparation of proton-exchange membranes of the fully sulfonated PSUs. Consequently, the three PSUs were also partly sulfonated in order to study the influence of the PSU structure on the water uptake characteristics and proton conductivity of the ionomer membranes.

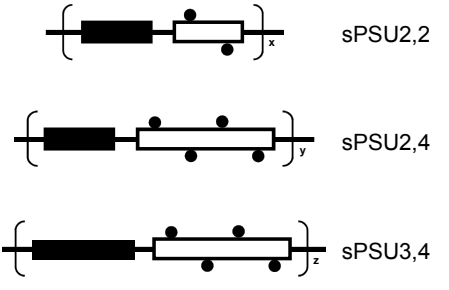

***Scheme 5.2**: A graphical illustration of the fully sulfonated PSU ionomers with varying lengths of the bisphenol (filled rectangles) and aryl sulfone segments (unfilled rectangles) with the sulfonic acid groups (filled circles) placed on the latter. The ionomers are designated as sPSUa,b, where a and b are the number of aryl rings in the repeating units that are linked by -C(CH$_3$)$_2$- and -SO$_2$- bridges, respectively.*

Preparation of the ionomers

Two PSUs, i.e., PSU2,4 and PSU3,4, were initially prepared via polycondensation reactions of bisphenol A and bisphenol P, respectively, together with 4,4'-bis[(4-chlorophenyl)sulfonyl]-1,1'-biphenyl (BCPSB). This led to PSUs with evenly spaced aryl-SO$_2$-aryl-aryl-SO$_2$-aryl segments along the polymer backbone.

In order to investigate the extent of modification that was possible, the two polymers were lithiated with a large excess of *n*-BuLi and were subsequently reacted with chlorotrimethylsilane in THF at -70 °C. The substitution of four positions per repeating unit was confirmed by ^{1}H NMR for both of the polymers.

After showing that it was possible to lithiate up to four positions per repeating unit of PSU2,4 and PSU3,4, it was explored whether one could synthesize fully sulfonated PSUs, i.e., with four sulfonic acid groups per repeating unit. In addition, PSU2,2 was also added to the study with the possibility of introducing two sulfonic acid groups per repeating unit, as previously shown by Kerres *et al.*[100] Fully sulfinated PSUs were prepared by reacting the polymers with a 25% excess of *n*-BuLi at -70 °C, followed by the addition of sulfur dioxide (Scheme 5.3), at which point the sulfinated product immediately precipitated from the THF solution.

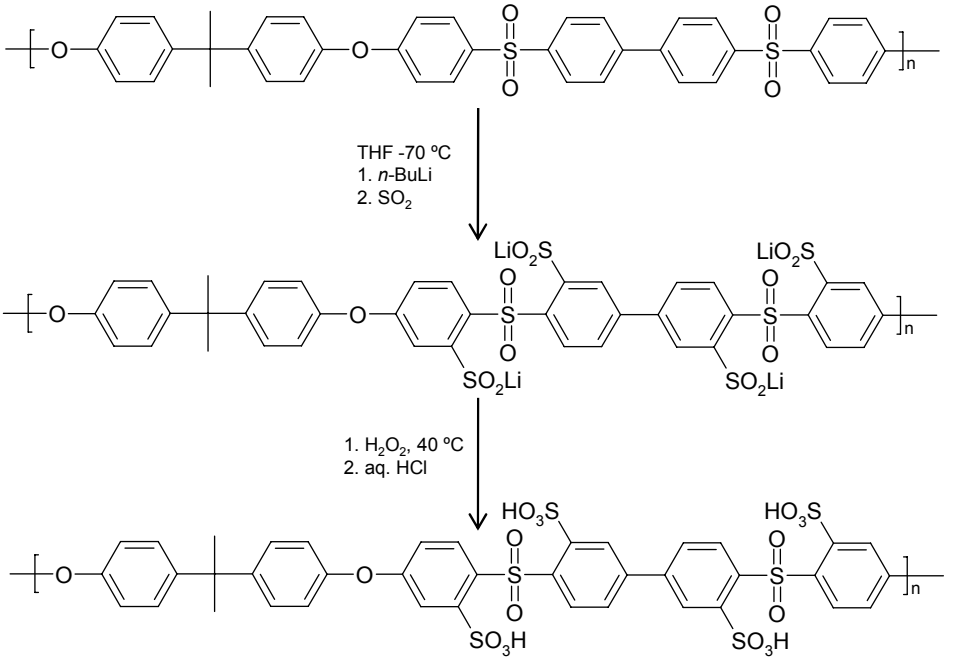

Scheme 5.3*: The sulfonation of PSU2,4 via lithiation and sulfination, followed by oxidation to obtain the fully tetrasulfonated derivative.*

The ^{1}H NMR spectra of the purified polymers, presented in Figure 5.3, confirmed the full sulfination, and the peak integrals all had the expected ratios. The sulfinated polymers were thereafter oxidized to the completely sulfonated polymers sPSU2,2-3.31, sPSU2,4-4.09, and sPSU3,4-3.65 by using hydrogen peroxide. The complete oxidation of all the sulfinates was confirmed by ^{1}H NMR as well as by Fourier transform infrared spectroscopy (FTIR), where the absorption band at 976 cm^{-1}, originating from the symmetrical S=O stretching of the sulfinate groups, was replaced by an absorption band at 1012 cm^{-1} originating from the symmetrical S=O stretching of the sulfonate groups.

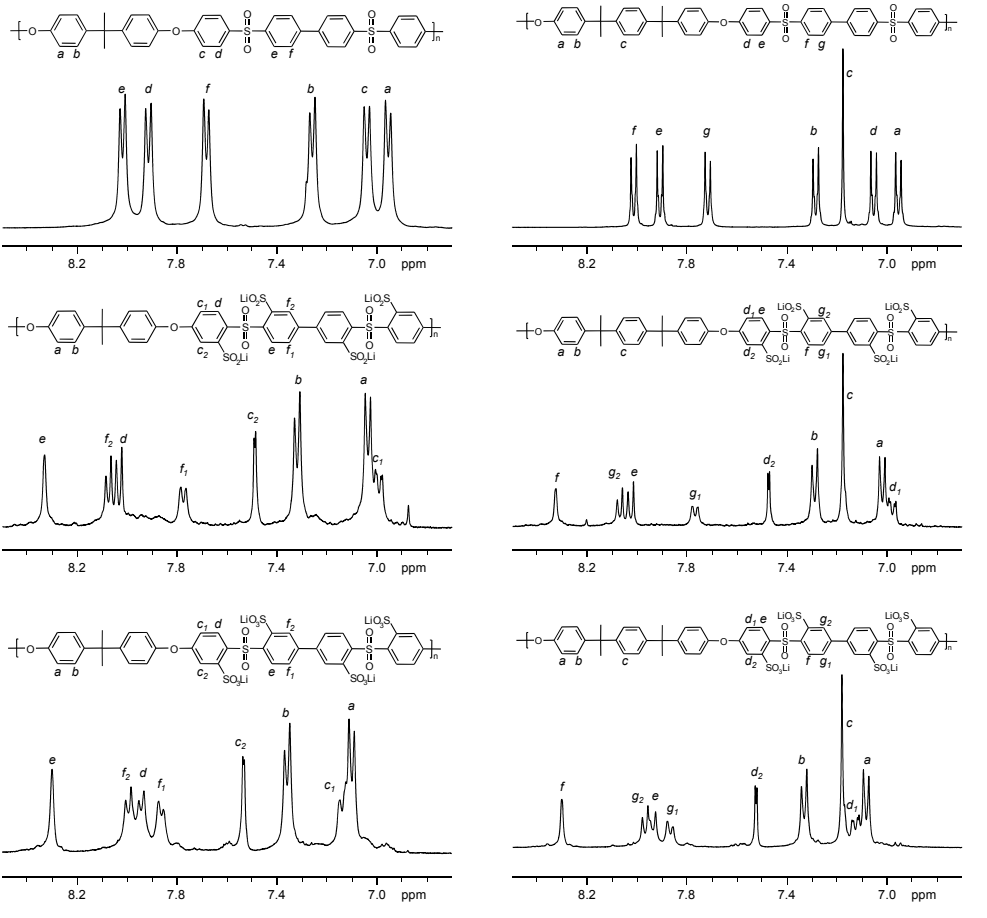

***Figure 5.3**: ^{1}H NMR spectra of the pristine, fully sulfinated, and fully sulfonated PSUs.*

Partly sulfinated polymers were prepared using a procedure similar to the one described for the fully sulfinated polymers, but with a smaller amount of *n*-BuLi. All the partly sulfonated PSUs were oxidized with the same method as that for the fully sulfonated PSUs and the complete oxidation was confirmed by both ^{1}H NMR and FTIR spectroscopies.

The degree of sulfination (DS) for all the ionomers was determined by ^{1}H NMR, through comparison of the signals arising from di- mono-, and non-sulfinated segments. The corresponding calculated IEC values, IEC_{calc}, ranged from 1.00 to 4.09 and were used to designate the IEC in the sample names. Unfortunately, due to peak overlap in the spectra of the partly sulfonated PSUs, the degree of sulfonation could not be determined from the ^{1}H NMR data.

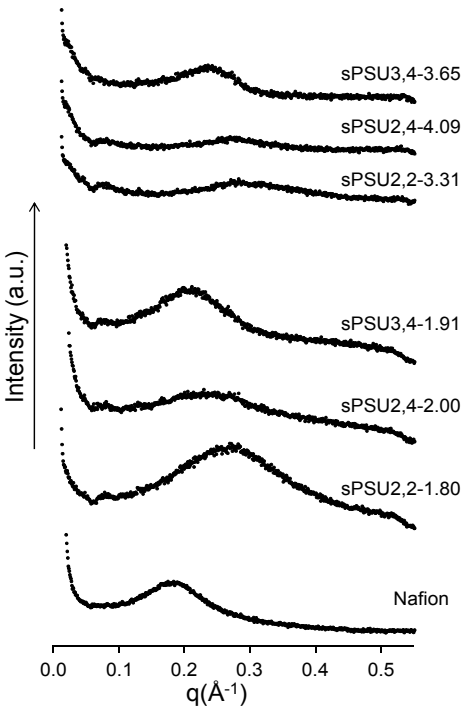

***Figure 5.4**: SAXS data on partly and fully sulfonated ionomer membranes having been ion-exchanged with lead acetate.*

Properties of the ionomers

The morphological features of the membranes were studied by SAXS on lead-ion exchanged membranes for which the contrast was enhanced by a selective staining of the ionic domains. The SAXS profiles originating from the six PSU ionomer membranes with the highest IEC values are shown in Figure 5.4 together with the corresponding profile of Nafion®. The profiles of the sulfonated PSU membranes displayed much broader ionomer peaks and were shifted to higher *q* values, as compared to the Nafion® profile. Their profiles indicated a smaller cluster separation, *d* = 22-30 Å, with a significantly wider distribution of the characteristic separation lengths. These findings are consistent with previously published SAXS data on dry main chain sulfonated aromatic polymers.[138-141] The profiles presented a shift to lower *q* values of the ionomer peak position for the polymers containing bisphenol P residues, in comparison to those containing bisphenol A residues.

This indicated that long flexible hydrophobic segments gave larger separation lengths between the ionic clusters, and thus promoted the ionic clustering process. Additionally, PSUs containing the larger sulfonated BCPSB residues exhibited lower q values as opposed to corresponding PSUs with DCDPS residues.

The thermal stability of the PEMFC membranes is a key property essential for the durability under fuel cell operation. This was investigated by thermogravimetrical analysis (TGA) by heating the membranes in their sodium salt form at 1 °C/min under air or 10 °C/min under N_2. The partly sulfonated PSUs were also investigated in their protonated form. The temperature at which the membranes retained 95 wt% of their initial weight, T_d, was shown to be higher for the ionomers based on the BCPSB monomer residue, sPSU2,4 and sPSU3,4, as compared to their sPSU2,2 counterpart. In the acid form, the T_d decreased significantly with increasing IEC values within all three series of ionomers. Partly sulfonated polymers with IECs of approximately 1.7 meq./g only decomposed above 240 °C during heating of 1 °C/min. under air. Notably, the T_d of all the ionomers were higher, by up to 70 °C under nitrogen, as compared to PSUs that had been post-sulfonated using trimethylsilyl chlorosulfonate,[93] or chlorosulfonic acid/chlorotrimethylsilane.[148] This indicated the advantage of using the lithiation-sulfonation reactions to introduce sulfonic acid on deactivated positions.

The fully sulfonated PSUs were water soluble. The partly sulfonated ionomers, on the other hand, were cast from DMAc solutions in the lithium salt form, resulting in tough transparent membranes, which were subsequently acidified. The water uptake of these party sulfonated PSU membranes was found to be low to moderate, ranging from 17 to 56%. Out of the three membranes in the narrow IEC range of approximately 1.7 meq./g, the water uptake of sPSU2,4 and sPSU3,4 was lower than that of sPSU2,2. The proton conductivity was measured under immersed conditions and was not surprisingly found to increase with an increase in IEC. In particular, conductivities above 0.1 S/cm at 80 °C were measured for the sPSU2,2 and sPSU2,4 membranes, which exceeded that of Nafion® over the entire temperature range studied.

The work presented in this paper demonstrated that BCPSB residues could be conveniently tetrasulfonated, thus offering possibilities to prepare various aromatic copolymers and membranes with locally very high densities of hydrolytically stable sulfonic acid groups. This should be beneficial for fuel cell operation under low RH conditions.

5.2 Polysulfones carrying sulfonated aromatic side chains (Paper II)

Paper II presents an investigation of PSUs carrying various aromatic mono-, di-, and trisulfonated side chains with respect to their nanoscale structure and key membrane properties. In order to increase the phase separation, the sulfonic acid groups were separated from the polymer backbone on short (sb) and longer (6snb and 7snb) side chains. Furthermore, the local concentration of the sulfonic acid groups was increased (dsnb and tspb). The molecular structures of the ionomers discussed in Paper II are shown in Scheme 5.4.

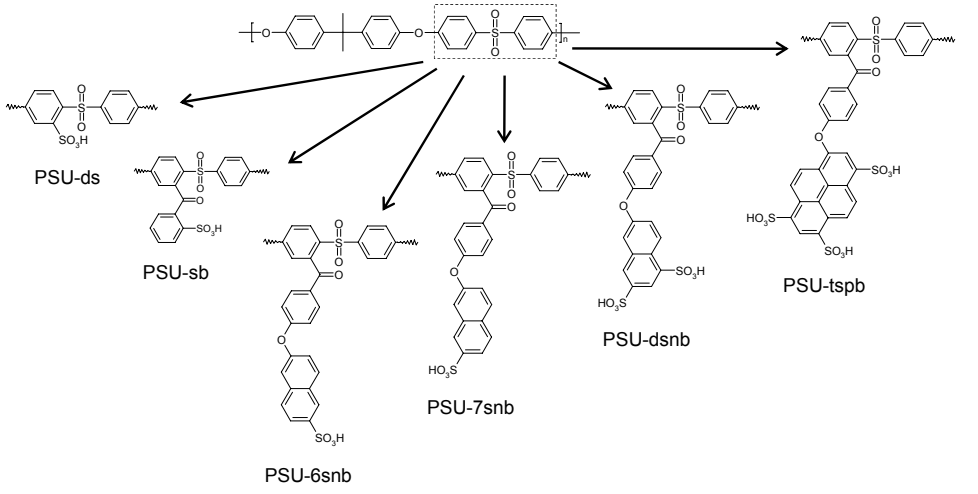

Scheme 5.4*: Molecular structures of the various sulfonated PSUs discussed in Paper II, from left to right, sulfonated (ds) PSU and PSU carrying sulfobenzoyl (sb), 6-sulfonaphthoxybenzoyl (6snb), 7-sulfonaphthoxybenzoyl (7snb), disulfonaphthoxybenzoyl (dsnb), and trisulfopyrenoxybenzoyl (tspb) side chains.*

All the ionomers from Paper II were synthesized via lithiation of a commercially available PSU. PSUs with longer sulfonaphtoxybenzoyl, disulfonaphtoxybenzoyl, and trisulfopyrenoxybenzoyl side chains were prepared from precursor polymers with highly activated fluorine atoms via nucleophilic aromatic substitution (S_NAr). The ionomers were all synthesized according to previously published methods,[73,75,76,100] but with minor modifications such as carrying out the dehydration of the hydroxyarylsulfonates in a separate step.

The morphology of the ionomer membranes was studied by SAXS and the obtained profiles are shown in Figure 5.5 together with those of Nafion® and backbone-sulfonated PSUs. As had also been observed in the SAXS profiles presented in

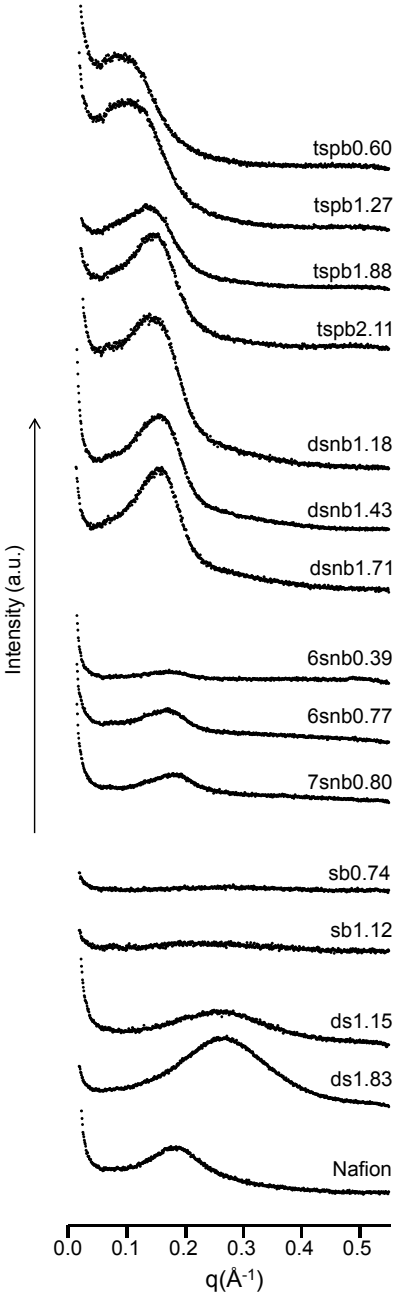

***Figure 5.5**: SAXS data recorded on dry polymer membranes ion-exchanged with lead acetate.*

Paper I, the backbone sulfonated PSUs showed much broader ionomer peaks shifted to higher q values, as compared to the profile of Nafion®. The PSUs functionalized with short side chains (sb) gave rise to very weak, hardly discernible, ionomer peaks. This could be explained by the position of the sulfonic acid units, *ortho* to the ketone link and close to the backbone, which may lead to a decreased mobility and steric shielding of the individual acid units during the membrane formation. The membranes based on the sulfonaphthoxybenzoyl (snb)-functionalized PSU, with extended side chains, clearly formed ionic clusters that gave rise to ionomer peaks with positions corresponding to $d \approx 37$ Å. The profiles were considerably narrower than those of the backbone-sulfonated PSUs. The disulfonaphthoxybenzoyl (dsnb)-functionalized PSU showed ionomer peaks having shifted to positions corresponding to d = 40-44 Å, depending on the IEC. The rather narrow peaks indicated that the clusters were quite uniformly distributed. The SAXS profiles of the PSUs functionalized with trisulfopyrenoxybenzoyl (tspb) side chains showed peak positions corresponding to d = 44-71 Å, depending on the IEC. As seen from the profiles of the PSUs with di- and trisulfonated side chains, the ionomer peaks shifted to lower d values when the IEC increased. This was consistent with the decrease in characteristic separation lengths resulting from the shorter distances between the ionic domains for membranes with increasing concentrations of sulfonic acid groups.

The water uptake of sulfonated polymer membranes has a profound effect on membrane conductivity and mechanical properties. Under immersed conditions, an increase in IEC expectedly led to an increase in water uptake, ranging from 12 to 104%. Figure 5.6a shows the water uptake as a function of the RH for a series of membranes with similar IEC values. As expected, all membranes showed a decrease in water uptake when the membranes were transferred from high to low RH at room temperature. At 35% RH, all membranes, except for the trisulfopyrenoxybenzoyl-functionalized membrane with the highest IEC, had comparable water uptake values of about 6%. Sulfonated aromatic polymers of similar IEC, including random, alternating, and multiblock copolymers, have previously been reported to reach water uptake values on the same level at low RH.[71]

Figure 5.6b shows the proton conductivity at different RH of the previously mentioned series of membranes with similar IEC values. The proton conductivity of the sulfobenzoyl side chain-bearing PSU decreased more than for the other membranes when the RH was lowered from 50 to 35%. This may indicate a faster loss of percolation in the pore system. On the contrary, the PSU bearing trisulfopyrenoxybenzoyl side chains showed a less significant decrease in the proton conductivity at lower RH, indicating water channels that were less sensitive to the loss of water. Despite that the PSU functionalized with disulfonaphthoxybenzoyl side chains presented the lowest water uptake at 35% RH, it nevertheless showed quite a high proton conductivity at this level of RH.

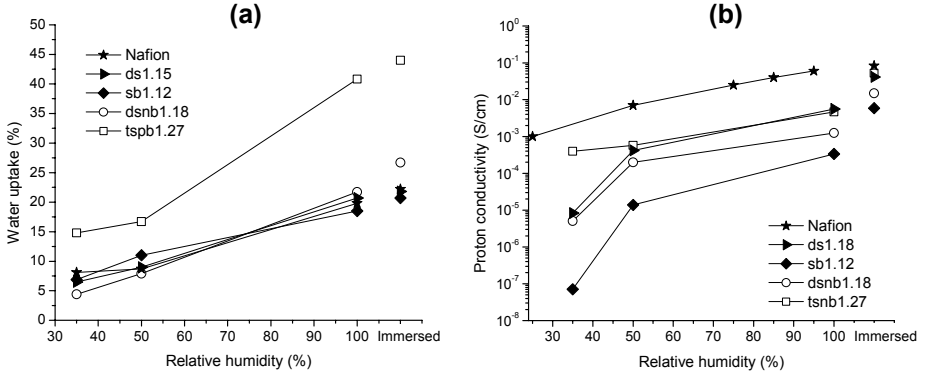

Figure 5.6*: (a) The water uptake and (b) proton conductivity of a series of ionomer membranes with similar IEC values as a function of RH. The data under immersed conditions are included for comparison. The proton conductivity data for Nafion® 117 at 20 °C were taken from reference.*[149]

The proton conductivity under immersed conditions was also studied for the series of membranes with similar IEC values. For the PSU bearing short sulfobenzoyl side chains, the proton conductivity was low, while it was higher for the PSU bearing disulfonaphthoxybenzoyl side chains. This was consistent with the more distinct ionomer peaks in the SAXS profiles. By further increasing the local acid concentration on the side chains, and hence also the characteristic separation length, with trisulfopyrenoxybenzoyl side chains, the level of proton conductivity was further increased to levels close to that of Nafion®.

The PSUs with sulfonaphthoxybenzoyl side chains differed in their levels of proton conductivity depending on the position of the sulfonic acid groups, despite their similar IEC values. The membrane based on the PSU functionalized with 6-sulfonaphthoxybenzoyl side chains gave a markedly higher proton conductivity compared with the membrane containing 7-sulfonapthoxybenoyl side chains, which notably also showed a markedly higher T_g.

The work presented in this paper demonstrated that the structure of the side chain could promote or depress the ionic clustering, as compared to the case of the backbone-sulfonated PSUs discussed in Paper I. The small separation between the polymer backbone and the sulfonic acid group present in the sulfobenzoyl side chain-bearing PSUs was not sufficient to enable an effective clustering. On the other hand, the measurements also revealed that, with longer side chains and higher local concentrations of sulfonic acid groups, the characteristic separation lengths between the ionic clusters increased. This observation was accompanied with narrower distributions, which indicated that the ions were efficiently clustered in the membranes. Proton conductivity measurements showed that larger characteristic separation lengths resulted in high proton conductivities, comparable to that of Nafion®.

5.3 Aromatic homopolymers and copolymers with pendant sulfonated side chains prepared by polycondensation reactions (Papers III-V)

Paper III describes the synthesis of a new monomer bearing fluorine atoms activated towards nucleophilic aromatic substitution. The reactivity and efficacy of this monomer was demonstrated by the preparation of a poly(arylene ether) and a poly(arylene ether sulfide) via polycondensation reactions. Paper IV presents the additional polymerizations of various diols to yield four poly(arylene ether)s and one poly(arylene ether ether sulfide) with similar IEC. The synthesis of another poly(arylene ether) is discussed in Paper V. Due to the high water uptake of the homopolymers presented in Papers III-V, copoly(arylene ether nitrile) and copoly(arylene ether sulfone) copolymers were prepared within the framework of Paper V with the aim to reduce the IEC and hence control the water uptake. The ionomers described in Papers III-V all had pendant sulfobenzoyl side chains that in Paper II were shown to give limited ionic clustering and thereby had low proton conductivities. Consequently, the influence of the polymer back-bone structure on the properties of the ionomers with sulfobenzoyl side chains was studied in Papers IV-V.

Preparation of the monomer

To prepare the lithium salt of 2,6-difluoro-2'-sufobenzophenone (DFSBP), 2-sulfobenzoic acid cyclic anhydride (SBACA) was added to 2,6-difluorophenyllithium in a one-pot synthesis according to Scheme 5.5. First, 1,3-difluorobenzene was lithiated with *n*-BuLi. Due to the strong *ortho*-directing power of the fluorine atoms, lithiation of 1,3-difluorobenzene occurred exclusively in the 2-position.[150] In the second step, SBACA was added to the lithiated compound. Ring-opening of the anhydride gave a lithium sulfonate group and a ketone link which deactivated the position of the sulfonate group and activated the fluorine atoms for nucleophilic aromatic substitution. During the reaction, the monomer crystallized out of the solution for which reason it was not necessary to salt out the product.

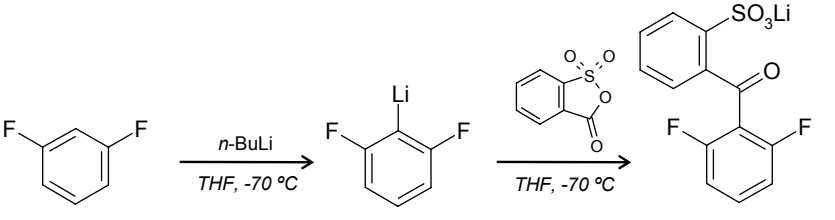

Scheme 5.5*: Synthesis of DFSBP.*

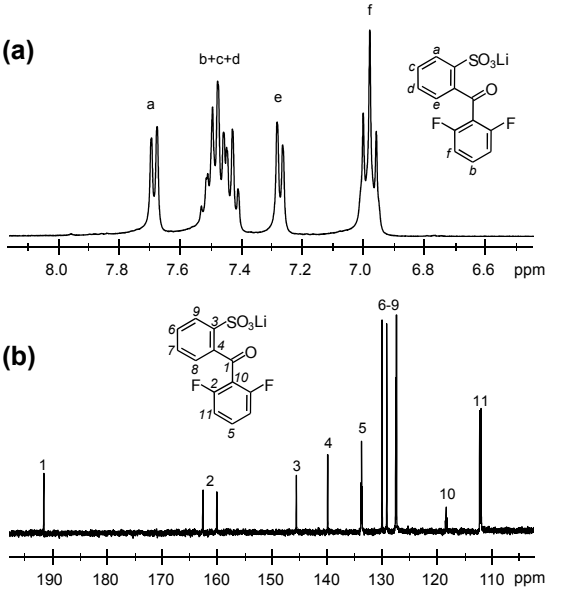

***Figure 5.7**: (a) [1]H and (b) [13]C NMR spectra of DFSBP recorded in DMSO-d_6 solution.*

The structure of recrystallized DFSBP was confirmed by ^{1}H and ^{13}C NMR spectroscopy (Figure 5.7). In the ^{13}C NMR spectrum, the resonance corresponding to the carbonyl carbon atoms could be found at δ = 191 ppm. Resonance attributed to the fluorinated carbon atoms were found at δ = 160.0 and 162.5 ppm.

Preparation of the ionomers

To obtain the homopolymers, DFSBP was polymerized via polycondensations in DMAc with seven diols and one dithiol, giving six poly(arylene ether)s (PAE, PAE1-4, and PAE2,6), one poly(arylene ether ether sulfide) (PAEES), and one poly(arylene sulfide) (PAS) as shown in Scheme 5.6. The diols were chosen to yield ionomers with polymer backbones of varying chemical nature and chain flexibility, but with similar IEC values. Similarly, the copolymers were prepared by polycondensations in DMAc with 2,7-dihydroxynaphthalene as the common diol. The IEC was controlled by varying the feed of DFSBP to 2,6-difluorobenzonitrile and bis[(4-fluorophenyl) sulfone], which yielded four copoly(arylene ether nitrile) (PAEN) and four copoly(arylene ether sulfone) (PAES), respectively (Scheme 5.7).

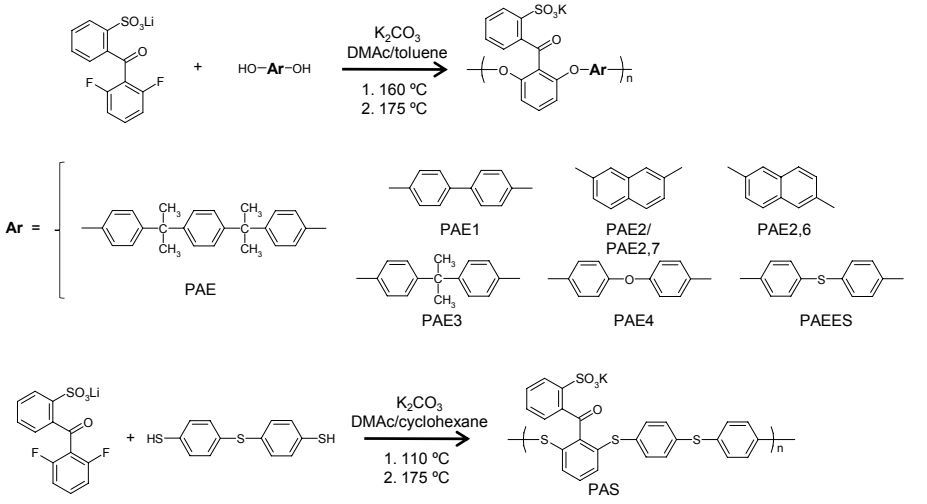

Scheme 5.6*: The synthetic pathway to the homopolymers presented in Papers III-IV.*

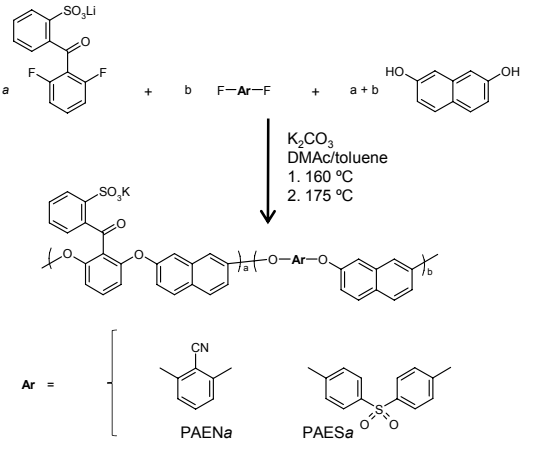

Scheme 5.7*: The synthetic pathway to the copolymers presented in Paper V.*

Ionomers were synthesized by mixing equimolar amounts of diols and activated aromatic fluorides together with a 25% of excess potassium carbonate. During the 4-h dehydration step, the reactants slowly precipitated, but regained solubility once toluene was completely removed. All homopolymers and copolymers of high IEC were found to precipitate during the polymerization, and the reaction temperature was consequently lowered to a temperature at which the polymers regained solubility. Solution viscosity measurements of ionomers were performed with DMSO

solutions with LiBr to avoid aggregation. Intrinsic viscosities were determined between 0.32 and 0.84 dLg^{-1}, as listed in Table 5.1. This indicated that moderate to high molecular weights were reached during the polymerization despite the precipitation of some of the ionomers.

The ionomers were characterized by means of ^{1}H NMR in DMSO-d_6 solutions. Integration of the resonances was in excellent agreement with the expected ionomer structures. The copolymers were additionally characterized by FTIR and the spectra are presented in Figure 5.8. The incorporation of the 2,6-difluorobenzonitrile and the bis[(4-fluorophenyl) sulfone] comonomers was confirmed by the appearance of a vibrational band at 2229 cm^{-1} originating from the nitrile triple bond stretch, and one at 1105 cm^{-1} corresponding to the S=O stretch in the sulfone linkage. The intensity of these bands increased with the proportion of non-sulfonated comonomer in the polymerization feed. In parallel, the vibrational bands at 1680 cm^{-1} and 1088 cm^{-1}, originating from the carbonyl stretch and S=O stretch in the sulfonic acid groups decreased in intensity.

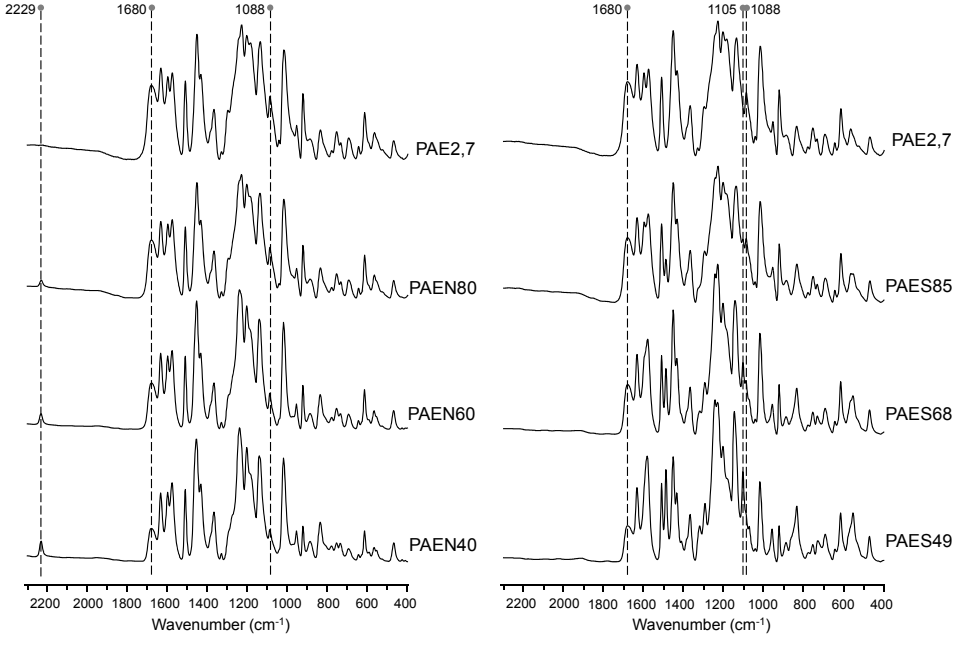

Figure 5.8*: FTIR spectra of the PAE2,7 homopolymer and the PAEN and PAES copolymers.*

Mechanically tough membranes were cast from NMP solutions of the ionomers as reported in Papers III-IV. In the study presented in Paper V, however, DMSO was chosen as the common solvent for membrane casting because of the full solubility of

all the included ionomers. Consequently, the PAE2/PAE2,7 ionomer, featured in both Paper IV and Paper V, was cast from two different solvents, NMP and DMSO, respectively, and was hence given different designations depending on the solvent used (Table 5.1). As opposed to the homopolymers discussed in Paper IV, the PAE2,6 homopolymer of Paper V was cast from DMSO, and a comparison of the membrane properties should thus be made with caution. The PAE membrane discussed in Paper III had a considerably lower IEC as opposed to the other homopolymers, and is therefore not included in the following section dealing with the properties of the polymers.

Properties of the polymers

As seen in Table 5.1, the homopolymers had similar IECs, while the structure of their polymer backbones differed. It was therefore anticipated that these materials would have dissimilar T_gs. The T_gs were also expected to differ among the co-polymers, but in this case as a consequence of their diverse IEC values. T_gs of the membranes in their sodium salt form are presented in Table 5.1. For the

***Table 5.1**: Selected membrane properties.*

Membrane	[η] (dLg^{-1})	IEC[c] (meq./g)	T_g[d] (°C)
PAE1[a]	0.41	2.22	300
PAE2[a]/PAE2,7[b]	0.84	2.25[a] /2.28[b]	n/d[a] / 300[b]
PAE2,6[b]	0.70	2.29[b]	334[b]
PAE3[a]	0.33	1.95	230
PAE4[a]	0.59	2.08	241
PAEES[a]	0.33	1.99	220
PAS[a]	0.59	1.87	252
PAEN80[b]	0.66	1.97	306
PAEN60[b]	0.43	1.55	266
PAEN40[b]	0.69	1.16	254
PAES85[b]	0.57	1.91	300
PAES68[b]	0.46	1.58	276
PAES49[b]	0.32	1.13	245

[a] Membrane cast from NMP
[b] Membrane cast from DMSO
[c] Measured by titration
[d] Measured in the sodium salt form
n/d: not detected

homopolymers, PAE3, PAE4, and PAEES showed the lowest T_gs (220 to 241 °C) due to their quite flexible polymer backbones, while PAE1 and PAS with their less flexible backbones presented T_gs of up to 300 °C. PAE2, cast from NMP, did not demonstrate any glass transition in the temperature range up to the onset of degradation at 400 °C. However, the same ionomer cast from DMSO, PAE2,7, showed a T_g of 300 °C, which indicated differences in membrane formation depending on the solvent used during casting. As was expected from its more extended backbone configuration, the PAE2,6 membrane exhibited an even higher T_g of 334 °C. The homopolymers with the highest T_g were found to be the most thermally stable under nitrogen atmosphere. As expected, the T_g declined with a decrease in IEC of the copolymers. This was consistent with the decrease in ionic sites, which lowered the intermolecular interactions and hence, increased the ionomer mobility. No difference in the level of T_g or thermal stability was found when comparing the two series of copolymers.

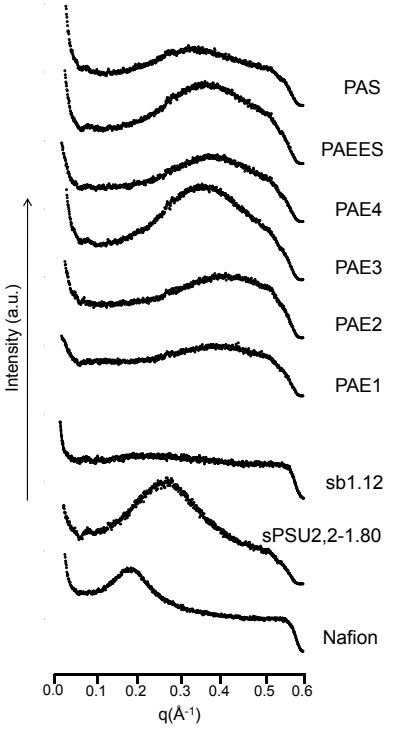

Figure 5.9*: SAXS data recorded using dry ionomer membranes having been ion-exchanged with lead acetate.*

The morphology of the homopolymer membranes cast from NMP was studied with SAXS. The SAXS profiles of the six ionomers are shown in Figure 5.9, together with the corresponding profile of Nafion®, the backbone-sulfonated sPSU2,2-1.80 from Paper I and a PSU bearing sulfobenzoyl side chains featured in Paper II. The membranes clearly formed ionic clusters with ionomer peak positions corresponding to d = 16-19 Å. The widths of the ionomer peaks were quite similar to those of backbone-sulfonated PSU. The positions of the peaks though differed greatly, showing smaller characteristic separation lengths between the ionic clusters in the ionomers bearing sulfobenzoyl side chains.

The T_g was found to have an influence on the SAXS profiles for the ionomers with similar IEC values. This was demonstrated by a weaker ionic clustering of the high-T_g ionomers PAE1, PAE2, and PAS, which all had rather stiff links in their polymer backbones in relation to the other ionomers. This apparently hindered the clustering of the ionic groups during membrane formation, possibly due to

restricted chain mobility. In contrast, the PAE3, PAE4, and PAEES ionomers, with lower T_g values and more flexible polymer backbones, demonstrated a more pronounced ionic clustering. As compared to the SAXS profile of the PSU bearing sulfobenzoyl side chains, the ionomer peaks of the membranes in this study demonstrated an improved ionic clustering, presumably because of the higher local chain flexibility around the sulfonic acid groups and due to higher IEC values. Yet, the ionomer peaks were still broad in comparison with the peak of Nafion®.

The IEC values of the homopolymers were elevated, which expectedly led to a considerable water uptake under immersed conditions, ranging from 73 to 627%, as seen in Figure 5.10a. The water uptake was found to increase with increasing IEC for the analogous series of PAE4, PAEES and PAS with the polymer backbone links of the repeating unit of three ether linkages, two ether linkages and one sulfide linkage, and three sulfide linkages, respectively. This trend indicated that the IEC, rather than the polymer backbone structure, was the main factor determining the water uptake within this series under immersed conditions.

The PAE1 membrane had a lower water uptake than expected from its high IEC. A possible explanation for this was the comparatively stiff polymer backbone which gave rise to a high T_g. The rigid PAE2 was found to take up excessive amounts of water under immersed conditions and also to swell unevenly, absorbing much more water at the edges as compared to in the center of the membrane. The PAE2,7 membrane, based on the identical ionomer but cast from DMSO, was found to have markedly lower water uptake levels than the PAE2 membrane cast from NMP, which indicated differences in the membrane formation depending on the solvent chosen. The water uptake of the PAE2,6 membrane was higher than for PAE2,7.

For the copolymers, the water uptake was expectedly found to decrease with a decrease in IEC, as seen in Figure 5.10b. There was a tendency for the PAEN copolymers to absorb less water than the PAES copolymers, which could be explained by the presence of the nitrile groups in the former membranes. These very polar groups were believed to increase the inter-chain molecular forces, and hence contribute to a reduction in water uptake. The reduction was nonetheless less significant than expected, possibly due to the relatively low concentrations of dissimilar parts of the copolymers.

When comparing the water uptake, under immersed conditions, of the PAEN40 and PAES49 membranes in this study with the backbone-sulfonated PSUs discussed in Paper I and the PSUs bearing sulfobenzoyl and disulfonaphthoxy side chains reported on in Paper II, all with IEC values of approximately 1.2, it was found that the water uptake was similar, within a narrow range of 21 to 27%.

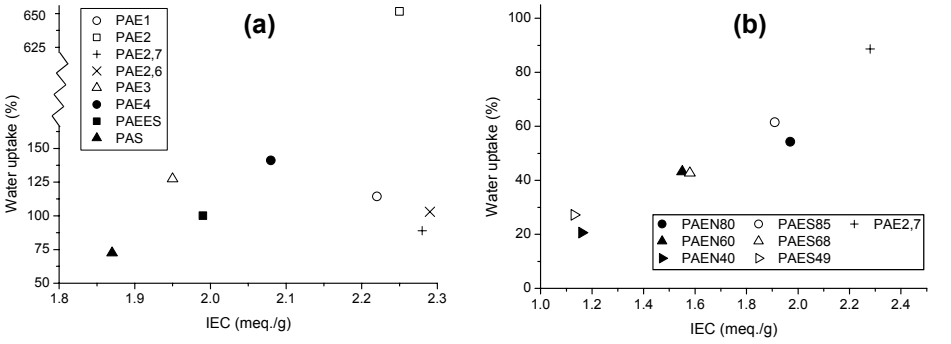

Figure 5.10*: The water uptake under immersed conditions at 25 °C for (a) the homopolymers and (b) the copolymers.*

The proton conductivity was studied by EIS in a sealed cell and is presented in Figure 5.11. Due to the high water uptake of the homopolymers described in Paper IV, the proton conductivity of these membranes was measured at 100% RH. These homopolymers had similar IEC values, and, as opposed to under immersed conditions, similar water uptake levels at 98% RH. As seen in Figure 5.11a, there was a tendency for the T_g to influence the proton conductivity. Consequently, the PAE1, PAE2, and PAS ionomers with stiff polymer backbones and high T_g were found to have the weakest proton conductivities, which was consistent with the less efficient ionic clustering in these membranes as observed by SAXS. Their high T_g presumably lowered the mobility and degree of freedom during the membrane formation process when the ionomer was in solution or in a solvent-swollen state, thus hindering a strong segregation and leading to a rather poor ionic clustering.[9] The solvent used for membrane casting was found to have a profound influence on the proton conductivity, as demonstrated by the difference in proton conductivity values between the PAE2 and PAE2,7 membranes.

The proton conductivity of the copolymers reported on in Paper V was measured by EIS under immersed condition. As seen in Figure 5.11b, the proton conductivity of the membranes with IEC values above 1.5 meq./g were all found within a narrow range. Despite their similar water uptake, the PAEN membranes had a tendency to present higher proton conductivities than their PAES counterparts in the previously mentioned IEC range. Not unexpectedly, the proton conductivity was found to drop markedly at lower IEC values. However, the PAEN40 and PAES49 membranes had proton conductivities similar to or exceeding that of the backbone-sulfonated PSU (Paper I) and the PSU bearing sulfobenzoyl side chains (Paper II). In addition, the PAES49 membrane had a proton conductivity in the same range as the PSU with disulfonaphthoxy side chains of similar IECs.

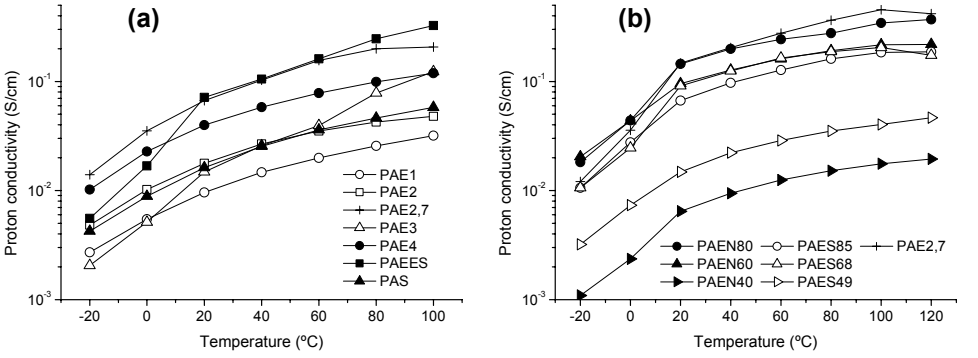

Figure 5.11*: Proton conductivity plots of (a) the homopolymers measured at 100% RH and (b) the copolymers measured under immersed conditions.*

The work in Papers III-V demonstrated that the T_g of the backbone influenced the ionic clustering during membrane casting, which in turn affected the proton conductivity attainable by the membranes at 100% RH. The ionic clustering was shown to be promoted by ionomers with flexible backbones and low T_g, resulting in higher proton conductivities, but with the drawback of lower thermal stabilities. The high water uptake of the homopolymers, was shown to be effectively restricted by the incorporation of non-sulfonated monomers to yield copolymers, but with the disadvantage of a lower proton conductivity. Nonetheless, at similar IEC values, these copolymers demonstrated higher proton conductivities than the PSUs bearing identical sulfobenzoyl side chains, indicating the influence of the backbone structure on membrane properties.

CHAPTER 6

SUMMARY AND OUTLOOK

Proton conductivity, water management, and thermal stability are properties that have an impact on the performance of the membrane in a fuel cell environment. These properties are all highly dependent on the molecular structure of the polymer membrane, and it is therefore of great importance to understand the connection between the molecular structure, morphology, water uptake, and proton conductivity in order to develop new proton-conducting membranes that satisfy the requirements of high proton conductivities at elevated operation temperatures.

For this purpose, the present thesis deals with the synthesis of a number of proton-exchange membranes with differing architectures, with the aim to enhance the phase separation between the hydrophilic acid-containing phase and the hydrophobic polymer backbone phase in order to improve the proton conductivity.

As a first strategy to enhance the phase separation, the sulfonic acid groups were concentrated to specific segments in the polymer backbone. PSUs with fully tetrasulfonated aryl-SO_2-aryl-aryl-SO_2-aryl segments were prepared by lithiation, reaction with sulfur dioxide, followed by oxidation of the resulting sulfinates. Although these polymers were water-soluble, the tetrasulfonated segments offered possibilities to prepare other aromatic copolymers and membranes with locally very high densities of hydrolytically stabile sulfonic acid groups.

As a second approach to enhance the phase separation, the sulfonic acid groups were separated from the polymer backbone and were concentrated to side chains. PSUs carrying various mono-, di-, and trisulfonated side chains were synthesized and the effects on the ionic clustering and properties were investigated. SAXS measurements revealed that with longer side chains and higher local acid concentrations, the characteristic separation length between the ionic clusters increased, and this was accompanied with a narrower distribution of separation lengths. Proton conductivity measurements showed that larger characteristic separation lengths resulted in higher proton conductivities. PSUs bearing sulfobenzoyl side chains were found to

give suppressed ionic clustering, and based on these observations, the influence of the polymer backbone structure was studied.

Polycondensation reactions were employed to synthesize aromatic ionomers of various polymer backbones with pendant sulfobenzoyl side chains. The ionic clustering was shown to be promoted by ionomers with flexible polymer backbones, which in turn gave rise to higher proton conductivities, but with the drawback of lower thermal stabilities. These ionomers had too high water uptake levels for practical use as proton-exchange membranes. As a consequence, copolymers in which the sulfonated monomers were diluted with non-sulfonated ones were prepared by polycondensation reactions. The obtained copolymers demonstrated a lower water uptake but, as a consequence, also lower proton conductivities. Nevertheless, at similar IEC values, these copolymers possessed higher proton conductivities than the PSUs bearing identical sulfobenzoyl side chains, indicating an influence of the backbone structure on membrane properties.

Although a number of questions and connections regarding the structure-property relationships have been evaluated and discussed in this thesis, many aspects remain unsolved and require further investigation. Proton conductivity measurements performed under immersed or fully humidified conditions as well as SAXS measurements, performed on dry membranes, might lead to information regarding the connection between proton conductivity and membrane morphology being lost depending on the different humidification states of the studied membranes. For this reason, it would be beneficial to measure the proton conductivity under variable humidification and/or perform SAXS measurements on water-swollen membranes. Moreover, gas permeability and fuel cell test could further elucidate the suitability of the ionomers described in this thesis as proton-exchange membranes in fuel cells. It would also be interesting to study the mobility of the sulfonic acid groups in water-swollen membranes by solid state NMR. Moreover, much could be gained by further exploring the applications for the fully tetrasulfonated segment. Finally, the casting procedure and the casting solvent in particular, were found to have an influence on the water uptake and the proton conductivity of the membrane. This observation was only investigated and discussed briefly in this thesis. However, further studies dealing with the influence of the solvent casting procedure on the properties of the membranes could result in improved casting procedures, which might give rise to membranes with optimized properties.

POPULÄRVETENSKAPLIG SAMMANFATTNING

Växthuseffekten och klimatförändringar har de senaste decennierna påskyndat forskning och utveckling av alternativa energikällor, däribland bränslecellen. En första skiss på en bränslecell föddes redan på 1830-talet. Det dröjde dock till 1950-talet innan den första kommersiella bränslecellen användes i ett av NASAs projekt. I Sverige har forskning runt bränsleceller med långa kolkedjor, polymerer, (Polymer Electrolyte Membrane Fuel Cell, PEMFC) bedrivits sedan 1997 inom Mistras bränslecellsprogram.

Bränslecellen kan ses som ett mellanting av ett batteri och en förbränningsmotor. Liksom batteriet är bränslecellen en elektrokemisk process, där kemisk energi direkt omvandlas till elektrisk energi. Bränslet tillförs dock kontinuerligt likt en förbränningsmotor. Bränslet för en PEMFC bränslecell är vanligtvis vätgas. Hjärtat i bränslecellen är membranet, elektrolyten, vilken har flera uppgifter. Det ska separera elektroderna från varandra, transportera protoner mellan elektroderna, men samtidigt hindra elektroner och gasmolekyler att ta sig igenom. Membranet befinner sig i en aggressiv miljö med mekaniska påfrestningar, mycket sura förhållanden, höga temperaturer och dessutom med reaktiva molekyler närvarande. För att dagens membran ska leda protoner måste de dessutom vara fuktiga. Alla dessa egenskaper sätter mycket höga krav på det material som membranet består av. Idag används nästan uteslutande Du Ponts Nafion®, som i många fall utmärkt stämmer in på dessa krav. Det har dock begränsningar som gör att Nafion® i dagens form inte kan användas i nästa generations bränsleceller. Hur skiljer sig dagens och nästa generations bränsleceller åt? Ett mål, förutom att minska produktionskostnaden, är att höja driftstemperaturen, vilket kan ge många fördelar: protonledningen ökar samtidigt som bränslecellens katalysatorer tål större mängd orenheter i bränslet. Det är vid dessa förhöjda driftstemperaturer som Nafion® har sina begränsningar.

Att tillverka ett bra protonledande membran för bränsleceller är en stor utmaning – både tekniskt och vetenskapligt. Förbättras en egenskap innebär detta oftast att en annan egenskap försämras. Utvecklingen följs av många kompromisser. Typiska egenskaper som måste beaktas är kompromissen mellan vattenupptag och mekanisk stabilitet. Ett protonledande material som tar åt sig mycket vatten leder protoner bättre än ett material som tar åt sig lite vatten. Men, ju mer vatten som tas upp, desto mer sväller materialet och tappar mekanisk stabilitet. Drömmen är ett material

med hög protonledningsförmåga som samtidigt tar upp små eller måttliga mängder vatten. Hur mycket vatten ett protonledande membran tar upp är starkt sammankopplat med hur många syragrupper som finns i materialet, även kallat jonbyteskapacitet. En hög jonbyteskapacitet leder till högt vattenupptag. Men med ett effektivt vattenporsystem kan mängden vatten hållas nere utan att offra alltför mycket protonledningsförmåga.

Membranets kemiska struktur är mycket viktigt för att förstå hur vattenupptag, jonbyteskapacitet och prestanda hänger ihop. Nafion® består av en flexibel huvudkedja som modifierats med flexibla sidokedjor med syragrupper. Det är dessa sura, joniska grupper, som starkt samverkar med vatten och står för den protonledning som eftersöks i materialet. Huvudkedjan däremot, är starkt vattenavstötande. Att de olika delarna i samma molekyl har så olika egenskaper leder till att de sura grupperna samlas och bildar så kallade joniska kluster. När membranet läggs i vatten, eller utsätts för fukt, drar dessa joniska kluster åt sig vatten och bildar vattenfyllda porer i nanoskala.

För att undersöka hur ett bra vattenporsystem uppnås har vår forskargrupp tillverkat olika serier av polymerer där syragrupperna sitter på sidokedjor fästa på huvudkedjan. Protonledningsförmåga och storleken på jonklusterna har undersökts. Detta har visat att ju längre sidokedja och högre lokal koncentration av syragrupper polymeren har, desto större blir jonklusterna och därmed vattenkanalerna. De större vattenkanalerna har i sin tur visat sig ge ökad protonledningsförmåga. I ett annat projekt har vi tillverkat polymerer där syragrupperna sitter på sidokedjor, men där huvudkedjorna har olika styvhet och kemisk struktur. De polymerer som hade flexibla huvudkedjor visade sig leda protoner bättre, men hade tyvärr sämre motståndskraft mot värme.

Vi har vidare studerat polymerer med syragruppen placerade direkt på huvudkedjan. I dessa polymerer är syragrupperna jämnt fördelade längs huvudkedjan. Det har spekulerats i fördelar med att istället fästa syragrupperna tätt i vissa segment, separerade av segment helt utan syragrupper. Vi har framställt just sådana polymerer. Dessa har framställts från polymerer med segment som tillåter tät utplacering av syragrupper, separerade av segment som inte tillåter utplacering av syragrupper. Vi har med dessa polymerer visat att det är möjligt att fästa upp till fyra syragrupper per segment via så kallad metallorganisk kemi. Dessa material har i lågvinkelröntgenspridningsförsök visat sig anta en distinkt och regelbunden fasseparation mellan jonkluster och huvudkedjor.

ACKNOWLEDGEMENTS

Thanks to / Tack till

Patric, för utmärkt handledarskap och för allt du lärt mig. Det hade aldrig gått utan dig!

All my present and former colleagues at the Division for Polymer & Materials Chemistry. A special thanks to Anna, min kontorssambo och vän, jag saknar dig redan. Francois, for keeping the spirits up in the lab. Shogo, for introducing me to the world of polycondensations. Gunnel och Martin, för alla trevliga lunchstunder. Lasse S, för uppmuntran och engagemang. Fortsätt att kämpa på! Olle, för fint ledarskap.

Mina MISTRA-vänner, för ett gott samarbete.

Maria, Bodil och Truus, som så hjärtligt hjälp mig med allt mellan himmel och jord.

Limhamns brassband, för att ni får mig att slappna av åtminstone en gång i veckan.

Mina vänner, för härliga myskvällar, getter(!), och stunder för lösande av världsproblem – kommer vi någonsin fram till något?

Mina mor- och farföräldrar, som betyder så mycket.

Lillasyster Emma, som är så bra på att få mig att tänka på annat.

Mamma och Pappa, för att ni alltid stöttar mig och för att ni gett mig bästa möjliga förutsättningar i Sveriges bästa skolor.

Min älskade man, Marcus, för att du alltid finns vid min sida och för att du engagerat dig i min forskning, trots att du egentligen inte gillar kemi…

Finally, the *Swedish Foundation for Strategic Environmental Research*, MISTRA, is gratefully acknowledged for financial support.

REFERENCES

1. M. L. Perry, T. F. Fuller, *J. Electrochem. Soc.* 2002, 149, S59-S67.
2. W. T. Grubb, L. W. Niedrach, *J. Electrochem. Soc.* 1960, 107, 131-135.
3. F. A. de Bruijn, V. A. T. Dam, G. J. M. Janssen, *Fuel Cells* 2008, 1, 3-22.
4. G. J. K. Acres, *J. Power Sources* 2001, 100, 60-66.
5. J. Zhang, Z. Xie, J. Zhang, Y. Tang, C. Song, T. Navessin, Z. Shi, D. Song, H. Wang, D. P. Wilkinson, Z.-S. Liu, S. Holdcroft, *J. Power Sources* 2006, 160, 872-891.
6. B. C. H. Steele, A. Heinzel, *Nature* 2001, 414, 345-352.
7. F. de Bruijn, *Green Chemistry* 2005, 7, 130-150.
8. M. Winter, R. J. Brodd, *Chem. Rev.* 2004, 104, 4245-4269.
9. K. D. Kreuer, *J. Membr. Sci.* 2001, 185, 29-39.
10. P. Jannasch, *Curr. Opin. Colloid Interface Sci.* 2003, 8, 96-102.
11. G. Alberti, M. Casciola, U. Costantino, R. Narducci, M. Pica, M. Sganappa, *Desalination* 2006, 199, 4-5.
12. Q. Li, R. He, J. O. Jensen, N. J. Bjerrum, *Chem. Mater.* 2003, 15, 4896-4915.
13. S. Licoccia, E. Traversa, *J. Power Sources* 2006, 159, 12-20.
14. O. Savadogo, *J.New Mat. Electrochem. Sys.* 1998, 1, 47-66.
15. K. A. Mauritz, R. B. Moore, *Chem. Rev.* 2004, 1004, 4535-4585.
16. S. Banerjee, D. E. Curtin, *J. Fluorine Chem.* 2004, 125, 1211-1216.
17. R. Souzy, B. Ameduri, *Prog. Polym. Sci.* 2005, 30, 644-687.
18. M. Casciola, G. Alberti, M. Sganappa, R. Narducci, *J. Power Sources* 2006, 162, 141-145.
19. M. C. Wintersgill, J. J. Fontanella, *Electrochim. Acta* 1998, 43, 1533-1538.
20. J. A. Kerres, *J. Membr. Sci.* 2001, 185, 3-27.
21. J. Rozière, D. J. Jones, *Annu. Rev. Mater. Res.* 2003, 33, 503-555.
22. M. A. Hickner, H. Ghassemi, Y. S. Kim, B. R. Einsla, J. E. McGrath, *Chem. Rev.* 2004, 104, 4587-4612.
23. A. L. Rusanov, P. V. Kostoglodov, M. J. M. Abadie, V. Y. Voytekunas, D. Y. Likhachev, *Adv. Polym. Sci.* 2008, 216, 125-155.

24. G. Maier, J. Meier-Haack, *Adv. Polym. Sci.* 2008, 216, 1-62.
25. T. Higashihara, K. Matsumoto, M. Ueda, *Polymer* 2009, 50, 5341-5357.
26. A. Eisenberg, *Macromolecules 1970, 3, 147-154.*
27. A. Eisenberg, B. Hird, R. B. Moore, *Macromolecules* 1990, 23, 4098-4107.
28. B. Hird, A. Eisenberg, *Macromolecules* 1992, 25, 6466-6474.
29. S. Gottesfeld, T. A. Zawodzinski, *Adv. Electrochem. Sci. Eng.* 1997, 5, 195-301.
30. Y. Yang, S. Holdcroft, *Fuel Cells* 2005, 5, 171-186.
31. B. Bae, K. Miyatake, M. Watanabe, *Macromolecules* 2009, 42, 1873-1880.
32. K.-D. Kreuer, S. J. Paddison, E. Spohr, M. Schuster, *Chem. Rev.* 2004, 104, 4637-4678.
33. A. Siu, J. Schmeisser, S. Holdcroft, *J. Phys. Chem. B* 2006, 110, 6072-6080.
34. Y. S. Kim, L. Dong, M. A. Hickner, T. E. Glass, V. Webb, J. E. McGrath, *Macromolecules* 2003, 36, 6281-6285.
35. K. Nakamura, T. Hatakeyama, H. Hatakeyama, *Polymer* 1983, 24, 871-876.
36. S. von Kraemer, A. I. Sagidullin, G. Lindbergh, I. Furó, E. Persson, P. Jannasch, *Fuel Cells 2*008, 8, 262-269.
37. K.-D. Kreuer, *Chem. Mater.* 1996, 8, 610-641.
38. C. A. Edmondson, P. E. Stallworth, M. E. Chapman, J. J. Fontanella, M. C. Wintersgill, S. H. Chung, S. G. Greenbaum, *Solid State Ionics* 2000, 135, 419-423.
39. N. Agmon, *Chem. Phys. Lett.* 1995, 244, 454-462.
40. K.-D. Kreuer, *Solid State Ionics* 2000, 136-137, 149-160.
41. M. E. Schuster, W. H. Meyer, *Annu. Rev. Mater. Sci.* 2003, 33, 233-261.
42. J. C. Persson, K. Josefsson, P. Jannasch, *Polymer* 2006, 47, 991-998.
43. H. Ghassemi, J. E. McGrath, T. A. Zawodzinski Jr., *Polymer* 2006, 47, 4132-4139.
44. X. Yu, A. Roy, S. Dunn, A. S. Badami, J. Yang, A. S. Good, J. E. McGrath, *J. Polym. Sci., Part A: Polym. Sci.* 2009, 47, 1038-1051.
45. K. Nakabayashi, K. Matsumoto, M. Ueda, *J. Polym. Sci., Part A: Polym. Chem.* 2008, 46, 3947-3957.
46. A. Roy, X. Yu, S. Dunn, J. E. McGrath, *J. Membr. Sci.* 2009, 327, 118-124.
47. K. Nakabayashi, K. Matsumoto, M. Ueda, *Polym. J.* 2009, 41, 332-337.
48. K. Nakabayashi, K. Matusmoto, M. Ueda, *J. Polym. Sci., Part A: Polym. Chem.* 2008, 46, 7332-7341.

49. H.-S. Lee, A. Roy, O. Lane, M. Lee, J. E. McGrath, *J. Polym. Sci., Part A: Polym. Chem.* 2010, 48, 214-222.
50. C. K. Shin, G. Maier, B. Andreaus, G. G. Sherer, *J. Membr. Sci.* 2004, 245, 147-161.
51. H.-S. Lee, A. S. Badami, A. Roy, J. E. McGrath, *J. Polym. Sci., Part A: Polym. Chem.* 2007, 45, 4879-4890.
52. B. Bae, T. Yoda, K. Miyatake, H. Uchida, M. Watanabe, *Angew. Chem. Int. Ed.* 2010, 49, 317-320.
53. K. Nakabayashi, T. Higashihara, M. Ueda, *J. Polym. Sci., Part A: Polym. Chem.* 2010, 48, 2757-2764.
54. A. Roy, M. A. Hickner, X. Yu, Y. Li, T. E. Glass, J. E. McGrath, *J. Polym. Sci., Part B: Polym. Phys.* 2006, 44, 2226-2239.
55. A. Mokrini, J. L. Acosta, *Polymer* 2001, 42, 8817-8824.
56. C. A. Martinez, A. S. Hay, *Polymer* 2002, 43, 5807-5817.
57. K. Matsumoto, T. Higashihara, M. Ueda, *Macromolecules* 2008, 41, 7560-7565.
58. B. Gupta, F. N. Büchi, M. Staub, D Grman, G. G. Scherer, *J. Polym. Sci., Part A: Polym. Chem.* 1996, 34, 1873-1880.
59. N. Walsby, F. Sundholm, T. Kallio, G. Sundholm, *J. Polym. Sci., Part A. Polym. Chem.* 2001, 39, 3008-3017.
60. M. Elomaa, S. Hietala, M. Paronen, N. Walsby, K. Jokela, R. Serimaa, M. Torkkeli, T. Lehtinen, G. Sundholm, F. Sundholm, *J. Mater. Chem.* 2000, 10, 2678-2684.
61. T. B. Norsten, M. D. Guiver, J. Murphy, T. Astill, T. Navessin, S. Holdcroft, B. L. Frankamp, V. M. Rotello, J. Ding, *Adv. Funct. Mater.* 2006, 16, 1814-1822.
62. J. Ding, C. Chuy, S. Holdcroft, *Chem. Mater.* 2001, 13, 2231-2233.
63. J. Ding, C. Chuy, S. Holdcroft, *Macromolecules* 2002, 35, 1348-1355.
64. S. Matsumura, A. R. Hlil, C. Lepiller, J. Gaudet, D. Guay, A. S. Hay, *Macromolecules* 2008, 41, 277-280.
65. S. Matsumura, A. R. Hlil, C. Lepiller, J. Gaudet, D. Guay, Z. Shi, S. Holdcroft, A. S. Hay, *Macromolecules* 2008, 41, 281-284.
66. S. Matsumura, A. R. Hlil, N. Du, C. Lepiller, J. Gaudet, D. Guay, Z. Shi, S. Holdcroft, A. S. Hay, *J. Polym. Sci., Part A: Polym. Chem.* 2008, 46, 3860-3868.
67. S. Tian, Y. Meng, A. S. Hay, *Macromolecules* 2009, 42, 1153-1160.
68. K. Matsumoto, T. Higashihara, M. Ueda, *Macromolecules* 2009, 42, 1161-1166.

69. S. Matsumoto, T. Higashihara, M. Ueda, *J. Polym. Sci., Part A: Polym. Chem.* 2009, 47, 3444-3453.
70. Z. Zhu, N. M. Walsby, H. M. Colquhoun, D. Thompsett, E. Petrucco, *Fuel Cells* 2009, 4, 305-317.
71. M. L. Einsla, Y. S. Kim, M. Hawley, H.-S. Lee, J. E. McGrath, B. J. Liu, M. D. Guiver, B. S. Pivovar, *Chem. Mater.* 2008, 20, 5636-5642.
72. P. Jannasch, *Fuel Cells* 2005, 5, 248-260.
73. B. Lafitte, L. E. Karlsson, P Jannasch, *Macromol. Rapid Commun.* 2002, 23, 896-900.
74. L. E. Karlsson, P. Jannasch, *Electrochim. Acta* 2005, 50, 1939-1946.
75. B. Lafitte, M. Puchner, P. Jannasch, *Macromol. Rapid Commun.* 2005, 26, 1464-1468.
76. B. Lafitte, P. Jannasch, *Adv. Funct. Mater.* 2007, 17, 2823-2834.
77. L. Wang, S. Xiang, G. Zhu, *Chem. Lett.* 2009, 38, 1004-1005.
78. L. E. Karlsson, P. Jannasch, *J. Membr. Sci.* 2004, 230, 61-70.
79. J. Pang, H. Zhang, X. Li, L. Wang, B. Liu, Z. Jiang, *J. Membr. Sci.* 2008, 318, 271-279.
80. J. Zhu, K. Shao, G. Zhang, C. Zhao, Y. Zhang, H. Li, M. Han, H. Lin, D. Xu, H. Yu, H. Na, *Polymer* 2010, 51, 3047-3053.
81. X. Glipa, M. El Haddad, D. J. Jones, J. Rozière, *Solid State Ionics* 1997, 97, 323-331.
82. T. Yasuda, Y. Li, K. Miyatake, M. Hirai, M. Nanasawa, M. Watanabe, *J. Polym. Sci., Part A: Polym. Chem.* 2006, 44, 3995-4005.
83. J. Saito, K. Miyatake, M. Watanabe, *Macromolecules* 2008, 41, 2415-2420.
84. T. Mikami, K. Miyatake, M. Watanabe, *ACS Appl. Mater. Interfaces* 2010, 2, 1714-1721.
85. P. T. McGrail, *Polym. Int.* 1996, 41, 103-121.
86. V. L. Rao, *J. Macromol. Sci. Rev. Macromol. Chem. and Phys.* 1999, C39, 655-711.
87. C. Iojoiu, M. Maréchal, F. Chabert, J.-Y. Sanchez, *Fuel Cells* 2005, 5, 344-354.
88. J. F. Blanco, Q. T. Nguyen, P. Schaetzel, *J. Polym. Sci., Part A: Polym. Chem.* 2002, 84, 2461-2473.
89. A. Noshay, L. M. Robeson, *J. Appl. Polym. Sci.* 1976, 20, 1885-1903.
90. M. B. Cinderey, J. B. Rose, *Eur. Pat. Appl. EP 29633 A2 19810603* 1981.
91. M. J. Coplan, G. Götz, *U.S. Pat. 4.273.903* 1983.
92. C.-M. Bell, R. Deppisch, H. J. Golh, *U.S. Pat. 5.401.410* 1995.

93. S. Guhathakurta, K. Min, *J. Appl. Polym. Sci.* 2010, 115, 2514-2522.
94. C. Vogel, J. Meier-Haack, A. Taeger, D. Lehmann, *Fuel Cells, 2004, 4, 320-327.*
95. M. Schuster, K.-D. Kreuer, H. T. Andersen, J. Maier, *Macromolecules* 2007, 40, 598-607.
96. R. Nolte, K. Ledjeff, M. Bauer, R. Mülhaupt, *J. Membr. Sci.* 1993, 83, 211-220.
97. T. W. Beihoffer and J. E. Glass, *Polymer* 1986, 27, 1626-1632.
98. M. D. Guiver, J. W. ApSimon, O. Kutowy, *J. Polym. Sci., Part C: Polym. Lett.* 1988, 83, 211-220.
99. M. D. Guiver, J. W. ApSimon, O. Kutowy, *U.S. Patent 4,833,219* 1989.
100. J. Kerres, W. Cui, S. Reichle, *J. Polym. Sci., Part A: Polym. Chem.* 1996, 34, 2421-2438.
101. J. Kerres, W. Zhang, W. Cui, *J. Polym. Sci., Part A: Polym. Chem.* 1998, 36, 1441-1448.
102. B. Lafitte, P. Jannasch, *J. Polym. Sci., Part A: Polym. Chem.* 2006, 45, 269-283.
103. J. Parvole, P. Jannasch, *J. Mater. Chem.* 2008, 18, 5547-5556.
104. J. Parvole, P. Jannasch, *Macromolecules* 2008, 41, 3893-3903.
105. R. N. Johnson, A. G. Farnham, R. A. Clendinning, W. F. Hale, C. N. Merriam, *J. Polym. Sci., Part A-1: Polym. Chem.* 1967, 5, 2375-2398.
106. T. E. Attwood, P. C. Dawson, J. L. Freeman, L. R. J. Hoy, J. B. Rose, P. A. Staniland, *Polymer* 1981, 22, 1096-1103.
107. T. E. Attwood, A. B. Newton, J. B. Rose, *British Polymer J.* 1972, 4, 391-399.
108. H. R. Kricheldorf, G. Bier, *Polymer* 1984, 25, 1151-1156.
109. H. R. Kricheldorf, G. Bier, *J. Polym. Sci., Polym Chem. Ed.* 1983, 21, 2283-2289.
110. J. B. Rose, British Patent 1.414.421.
111. H. M. Colquhoun, C. C. Dudman, D. J. Blundell, A. Bunn, P. D. Mackenzie, P. T. McGrail, E. Nield, J. B. Rose, D. J. Williams, *Macromolecules* 1993, 26, 107-111.
112. V. Carlier, B. Jambe, J. Devaux, R. Legras, P. T. McGrail, *Polymer* 1993, 34, 167-170.
113. F. Wang, M. Hickner, Q. Ji, W. Harrison, J. Mecham, T. A. Zawodzinski, J. E. McGrath, *Macromol. Symp.* 2001, 175, 387-395.

114. F. Wang, M. Hickner, Y. S. Kim, T. A. Zawodzinski, J. E. McGrath, *J. Membr. Sci.* 2002, 197, 231-242.
115. W. L. Harrison, F. Wang, J. B. Mecham, V. A. Bhanu, M. Hill, Y. S. Kim, J. E. McGrath, *J. Polym. Sci., Part A: Polym. Chem.* 2003, 2264-2276.
116. B. Bae, K. Miyatake, M. Watanabe, *J. Membr. Sci.* 2008, 310, 110-118.
117. M. J. Sumner, W. L. Harrison, R. M. Weyers, Y. S. Kim, J. E. McGrath, J. S. Riffle, A. Brink, M. H. Brink, *J. Membr. Sci.* 2004, 199-211.
118. K. B. Wiles, C. M. deDiego, J. de Abajo, J. E. McGrath, *J. Membr. Sci.* 2007, 294, 22-29.
119. D. J. Yoo, S. H. Hyun, A. R, Kim, G. G. Kumar, K. S. Nahm, *Polym. Int.* 2010, DOI: 10.1002/pi.2914.
120. R. T. S. Muthu Lakshmi, J. Meier-Haack, K. Schlenstedt, C. Vogel, V. Choudhary, I. K. Varma, *J. Membr. Sci.* 2005, 261, 27-35.
121. H. Li, Z. Cui, C. Zhao, J. Wu, T. Fu, Y. Zhang, K. Shao, H. Zhang, H. Na, W. Xing, *J. Membr. Sci.* 2009, 164-170.
122. P. Xing, G. P. Robertson, M. D. Guiver, S. D. Mikhailenko, S. Kaliaguine, *J. Polym. Sci., Part A: Polym. Chem.* 2004, 42, 2866-2876.
123. J. Li, H. Yu, *J. Polym. Sci., Part A: Polym. Chem.* 2007, 45, 2273-2286.
124. Y. Gao, G. P. Robertson, M. D. Guiver, G. Wang, X. Jian, S. D. Mikhailenko, X. Li, S. Kaliaguine, *J. Membr. Sci.* 2006, 278, 26-34.
125. C. Zhao, X. Li, H. Lin, K. Shao, H. Na, *J. Appl. Polym. Sci.* 2008, 108, 671-680.
126. Y. Gao, G. P. Robertson, M. D. Guiver, S. D. Mikhailenko, X. Li, S. Kaliaguine, *Polymer,* 2006, 47, 808-816.
127. Y. Gao, G. P. Robertson, M. D. Guiver, S. D. Mikhailenko, X. Li, S. Kaliaguine, *Macromolecules* 2005, 38, 3237-3245.
128. Y. Gao, G. P. Robertson, D.-S. Kim, M. D. Guiver, S. D. Mikhailenko, X. Li, S. Kaliaguine, *Macromolecules* 2007, 40, 1512-1520.
129. D. S. Kim, G. P. Robertson, M. D. Guiver, Y. M. Lee, *J. Membr. Sci.* 2006, 281, 111-120.
130. G. Gebel, O. Diat, *Fuel Cells* 2005, 5, 261-276.
131. R Longworth, D. J. Vaughan, *Polym. Prep. (Am. Chem. Soc., Div. Polym. Chem.)* 1968, 9, 525-533.
132. J. Kao, R. S. Stein, W. J. MacKnight, W. P. Taggart, G. S. Cargill, *Macromolecules* 1974, 7, 95-100.
133. C. L. Marx, D. F. Caufield, S. L. Cooper, *Macromolecules* 1973, 6, 344-353.
134. D. J. Yarusso, S. L. Cooper, *Polymer* 26, 371-378.

135. D. J. Yarusso, S. L. Copper, *Macromolecules* 16, 1871-1880.
136. T. D. Gierke, G. E. Munn, F. C. Wilson, *J Polym Sci, Polym Phys* 1981, 19, 1687-1704.
137. G. Gebel, *Polymer* 2000, 41, 5829-5838.
138. D. X. Luu, E.-B. Cho, O. H. Han, D. Kim, *J. Phys. Chem. B 2009,* 113, 10072-10076.
139. B. Yang, A. Manthiram, *J. Power Sources* 2006, 153, 29-35.
140. N. Takimoto, L. Wu, A. Ohira, Y. Takeoka, M. Rikukawa, *Polymer* 2009, 50, 534-540.
141. M. A. Barique, L. Wu, N. Takimoto, K. Kidena, A. Ohira, *J. Phys. Chem. B, 2009,* 113, 15921-15927.
142. Miyatake, K.; Yasuda, T.; Hirai, M.; Nanasawa, M.; Watanabe, M. *J. Polym. Sci., Part A: Polym. Chem.* 2006, 45, 157-163.
143. Yoshimura, K.; Iwasaki, K. *Macromolecules* 2009, 42, 9302-9306.
144. C. H. Lee, H. B. Park, Y. M. Lee, R. D. Lee, *Ind. Eng. Chem. Res.* 2005, 44, 7617-7626.
145. B. D. Cahan, J. S. Wainright, *J. Electrochem. Soc.* 1993, 140, 185-186.
146. C. A. Edmondson, P. E. Stallworth, M. E. Chapman, J. J. Fontanella, M. C. Wintersgill, S. H. Chung, S. G. Greenbaum, *Solid State Ionics,* 2000, 135, 419-423.
147. S. D. Mikhailenko, M. D. Guiver, S. Kaliaguine, *Solid State Ionics*, 2008, 179, 619-624.
148. H. B. Park, H.-S. Shin, Y. M. Lee, J.-W. Rhim, J. Membr. Sci. 2005, 247, 103-111.
149. K. Tasaki, R. DeSousa, H.B. Wang, J. Gasa, A. Venkatesan, P, Pugazhendhi, R.O. Loutfy, *J. Membr. Sci.* 2006, 281, 570-580.
150. M. Schlosser, *Eur. J. Org. Chem.,* 2001, *21*, 3975-3984.